NASA SP-100

Significant Achievements in

Solar Physics

1958-1964

NASA SP-100

Significant Achievements in

Solar Physics 1958-1964

Scientific and Technical Information Division 1966
NATIONAL AERONAUTICS AND SPACE ADMINISTRATION
Washington, D.C.

FOR SALE BY THE SUPERINTENDENT OF DOCUMENTS, U.S. GOVERNMENT PRINTING OFFICE
WASHINGTON, D.C., 20402 - PRICE 50 CENTS

Foreword

THIS VOLUME IS ONE OF A SERIES which summarize the progress made during the period 1958 through 1964 in discipline areas covered by the Space Science and Applications Program of the United States. In this way, the contribution made by the National Aeronautics and Space Administration is highlighted against the background of overall progress in each discipline. Succeeding issues will document the results from later years.

The initial issue of this series appears in 10 volumes (NASA Special Publications 91 to 100) which describe the achievements in the following areas: Astronomy, Bioscience, Communications and Navigation, Geodesy, Ionospheres and Radio Physics, Meteorology, Particles and Fields, Planetary Atmospheres, Planetology, and Solar Physics.

Although we do not here attempt to name those who have contributed to our program during these first 6 years, both in the experimental and theoretical research and in the analysis, compilation, and reporting of results, nevertheless we wish to acknowledge all the contributions to a very fruitful program in which this country may take justifiable pride.

HOMER E. NEWELL
Associate Administrator for
Space Science and Applications, NASA

Preface

THE SUN IS A NATURAL OBJECT for the application of space technology. The importance of mapping its spectrum in the ultraviolet has long been recognized in establishing the presence of atoms not represented by spectral lines in the visible region, or in confirming tentative identifications based on faint subordinate lines in the visible. The response of the Earth's ionosphere to solar flare radiation raised a question of the nature of that radiation which could be directly answered by comparative observations of Lyman-alpha and X-radiation during flares and at quiet times. The emission lines of the corona, which are observed as forbidden transitions in the visible region, predicate permitted transitions of vastly increased strength in the extreme ultraviolet. The detection and measurement of these lines would permit a direct test of theories of excitation equilibrium processes in the corona. The spectral energy distribution in the Sun's extreme ultraviolet spectrum has to be known in order to interpret the state of excitation, ionization, and dissociation of atoms and molecules in the Earth's upper atmosphere. These are among the most familiar examples of problems of solar physics which attracted the attention of space scientists almost as soon as rocket technology became available for research in this country. Moreover, the highly variable and unpredictable character of solar activity, as, for example, solar flares, the corpuscular streams which produce sudden commencement distrurbances in the Earth's magnetosphere, and the coronal enhancements associated with the development of solar active regions, all created the need for continuity of observations of the Sun above the atmosphere, which only satellites could provide.

The study of the Sun from space vehicles must be viewed at all times in relation to the entire discipline of solar physics, which

utilizes a wide variety of distinct techniques of investigation. The theoretician utilizing large digital computers to study the constitution and evolution of the Sun, the radioastronomer who studies structures in the upper levels of the corona by observing occultations of radio stars, the laboratory spectroscopist who interprets the spectra of highly ionized light elements, and the amateur astronomer who counts sunspots as part of the international observing program, all these specialists contribute in their particular way to the general goals of solar physics. Particular interest in the Sun as the nearest and most readily observable star has resulted in a specialization of astronomical research since Galileo first counted and plotted sunspots. The peculiarities of instrumentation necessary to exploit the brilliance and propinquity of the Sun sometimes lead us to forget that solar physics is just a part of a broader field—stellar astrophysics. Similarly, space solar physics will at times be discussed apart from the whole discipline of diverse specialized techniques.

Astronomy differs from some branches of physics in the way we go about obtaining new knowledge and, indeed, in the kind of new knowledge we seek. For the Sun, particularly, the phenomena are so complex that a purely qualitative description of a phenomenon may be the closest we can get to a true understanding of the phenomenon. In this respect the study of solar activity is like the study of terrestrial weather. The parallel has a further application—both sciences deal with unpredictable events, and so require continuous monitoring observations to secure needed data for research. The ideal of some sciences, to relate complicated observations to a simple physical theory (for example, by demonstrating that the observed boundary conditions are compatible with a simple differential equation), often cannot be achieved in solar astronomy. Some of the most gratifying advances made in solar physics have indeed been the discovery that complicated things have simple explanations: for example, the identification of the coronal emission lines, and the interpretation of sunspot motions as the migration of magnetic current systems from high to low latitudes during a double solar cycle. But all the outstanding problems of solar physics, insofar as they have been resolved, have merely raised other more diffi-

cult questions: Why is the corona so hot that it produces very highly ionized iron and calcium atoms? Why do subphotospheric magnetic current systems exist, why do they migrate toward the Equator, and why does a 22-year cycle characterize their motions?

A very large part of the work of a solar astronomer in the space program consists of extending to the ultraviolet and X-ray region observations which are classical in the visible spectrum and whose importance was recognized decades ago. There is another respect in which the tasks of space solar astronomy are obvious to the specialist. Progress has to be made in orderly steps of increasing resolution, corresponding in a rough way to the scale of the solar structures of interest. These range from active regions up to a few minutes of arc in size; through flares and sunspots, of the order of a few tens of seconds of arc, and the granulation and network, ranging between 1 second and half a minute of arc; down to the smallest structures we know, including the fiber structures of prominences, chromospheric spicules, and the smallest components of the granulation. The most critical research problems in the repertoire of solar astronomy can thus be sketched out in considerable detail by a direct translation of visible light phenomena into the ultraviolet and X-ray wavelengths. Furthermore, the research requirements can be set out years in advance of technology. Consequently, the solar astronomer is well able to lay out a plan of several generations of space research vehicles, confident he can make justifiable use of each in a rational time scale.

Contents

Chapter 1

Background

A POWERFUL NEW TOOL became available to the astronomer in the form of V–2 rockets, and its most obvious application was to solar studies. The first objective was to chart the Sun's ultraviolet spectrum below the atmospheric window cutoff at about 2910 angstroms. Mapping of the solar ultraviolet spectrum has continued up to the present and probably will never be complete as long as wavelength resolution or the combination of wavelength and angular resolution can be improved. A second type of rocket-borne experiment measured the spectral distribution of solar radiation. Interest in the Sun's far ultraviolet has been stimulated by theoretical models of the Earth's upper atmosphere and ionosphere. Such models must assume an intense and highly variable source of solar ionizing radiation. Either hydrogen Lyman-alpha, the resonance radiation of the most abundant element in the Sun, or X-rays had to be invoked to account for some of the principal characteristics and variations of the ionosphere. The identity of this ionizing radiation remained an object of speculation and debate until rocket observations finally settled the question during the International Geophysical Year (IGY).[1]

Since these initial explorations of the Sun's far-ultraviolet and X-ray spectra, our knowledge has increased considerably. The purpose of this review is to cite the advances in solar astronomy made possible since the IGY by space research techniques. This time period overlaps the history of the National Aeronautics and Space Administration. However, the review will not be confined to NASA efforts. Much of the research reviewed was performed by laboratories of other agencies, notably the Air Force Cambridge Research Laboratory (AFCRL) and the Naval Research Laboratory (NRL). Part of this space research by other

Government agencies was of course, sponsored and supported by NASA.

To set the stage for this review, it may be helpful to highlight the progress in solar research by rockets and satellites as reported at the General Assemblies of the International Astronomical Union in 1958. At the beginning of solar cycle 19 it was thought that the X-ray spectrum of the quiet Sun could be approximated by a half-million-degree blackbody distribution. This temperature implies that the X-ray spectrum has an effective short wave limit near 20 Å. When coronal condensations at a temperature of 2 million degrees were present however, the X-ray spectrum extended down to as low as 6 Å. During the preceding solar cycle (no. 18) the highest and lowest values of X-ray flux from the quiet Sun were 0.15 and 1 erg/cm^2/sec, respectively. In the spectral region between 1050 Å and 1350 Å, 90 percent of the total intensity results from hydrogen Lyman-alpha radiation. During solar cycle 18, fluxes ranged from 0.1 to 1.6 ergs/cm^2/sec. By 1958 intensities as high as 6 ergs/cm^2/sec had been detected. The NRL rocket program during the IGY had obtained flux measurements during flares of importance 1, 2, and 3, showing that X-ray emission below 8 Å was greatly increased, and probably extended down to 1 Å or 2 Å. Gradients in the continuous spectrum had been measured spectrophotometrically to wavelengths below 2200 Å and were found to correspond to an effective temperature of 5200°.

The Fraunhofer spectrum, which predominates down to about 2085 Å, had been mapped extensively. The Mg II doublet (2795 Å and 2803 Å) was recognized as the most important feature of this spectral region. A rocket-borne echelle grating spectrograph provided an effective resolution of 0.1 Å down to 2000 Å. The doubly reversed Mg II lines were shown to be very similar to the H and K lines of Ca II, except that the H_2 and K_2 components were stronger in Mg II.

Below 2085 Å the continuum intensity suddenly decreases, and the Fraunhofer lines become less distinct. To account for this, it was suggested that molecules such as NO and CO in the Sun's

atmosphere were acting as quasi-continuous absorbers. Between 2000 Å and 1500 Å, the solar spectrum was known to change from a continuum with Fraunhofer lines to a region where emission lines emerged above a rapidly weakening continuum. Rocket spectra in the range 1000 to 2000 Å, made in 1955 by both NRL and the group at the University of Colorado, revealed nearly all of the strong resonance lines of the most abundant elements in the Sun (hydrogen Lyman-alpha and Lyman-beta; He II; C I; C II; C III; C IV; N V; O I and O VI; Si II, Si III, Si IV; S II and P II). Certain expected lines were absent, such as the *raies ultimes* of N I, N II, and N III. Rense had made a single spectrum extending to much shorter wavelengths, including the resonance line of He II at 304 Å, and the He I resonance line at 584 Å.

The width of the hydrogen Lyman-alpha line was not known with certainty. One observation suggested that the line is as wide as 0.8 Å, another that it is no greater than 0.3 Å. Tentative hydrogen Lyman-alpha spectroheliograms were only partly successful and barely sufficient to indicate the general conformity between plages as shown by hydrogen Lyman-alpha, hydrogen Balmer-alpha, and calcium K-lines. Spectrograms made with a stigmatic spectrograph showed that limb brightening occurs in certain lines (C IV) and not in others (C I). The results were interpreted in terms of a simple, stratified, semitransparent atmosphere.

In short, much was known about the Sun's ultraviolet and X-ray spectrum by 1958. This report summarizes the progress made from 1958 to 1964.

chapter 2

The Frontiers of Solar Research

THE PRINCIPAL TASK OF SOLAR ASTRONOMY is to analyze the many kinds of electromagnetic radiation emitted by the Sun. This radiation must be observed at all wavelengths, including those to which the Earth's atmosphere is opaque. Thus solar telescopes, spectrographs, and other instruments must be carried above the atmosphere in rockets, satellites, and probes.

Some studies require continuous observations over days or months, as in studies of solar activity. These must ultimately use equipment carried in satellites which are independent of terrestrial meteorology and diurnal effects. Real-time monitoring of solar events will be supported by such satellites, which will telemeter data to ground stations.

Angular resolution of solar surface details is limited from the ground by atmospheric turbulence. By placing telescopes above the atmosphere, the theoretical limit of resolution for a perfect lens or mirror can be attained.

Another reason for observing the Sun from rockets and satellites is atmospheric scattering. The inhomogeneities and dust of the atmosphere scatter the Sun's disk light, making it impossible to see the outer solar corona, the zodiacal light, or the gegenschein free of contamination. Space platforms, being above the scattering layers, are not subject to this disadvantage.

Radiofrequency observations of any celestial source below about 10 Mc/sec must be conducted above the interfering layers of the Earth's ionosphere. The electrically conducting plasma in the upper atmosphere absorbs completely the solar radio emission below a critical frequency which diminishes with height. Even above the critical frequency for ground observations, large-scale irregularities and time variations in the ionosphere produce scintillation (fluctuation) in solar radio emission observed from

the ground, which masks solar phenomena. Low-frequency ground observations of cosmic radio noise are much confused by terrestrial transmissions, which are scattered and reflected downward by the ionosphere, so that an orbiting low-frequency solar radio telescope will also benefit from diminished background noise.

To describe the present state of knowledge and the major areas of interest, some of the frontiers of solar research will be dealt with from the standpoint of the space astronomer as well as his colleagues who view from the ground.

SOLAR ACTIVITY

Neither the origin nor the effects of the time variation of solar processes are well understood. Nearly every true statement about solar activity can be properly rephrased as a question. We know that solar activity varies over an 11-year period but cannot show how this period results from boundary conditions. One goal of the solar astronomer is to discover the relation of the Sun's basic parameters (diameter, luminosity, composition, age, and rotation) to the time and energy scales of solar activity. Another unexplained phenomenon is the familiar migration of centers of activity from middle latitudes toward the Equator during the 11-year cycle. The outstanding tasks of this discipline include solving the following problems:

(1) What causes solar flares?
(2) How are solar protons accelerated and expelled?
(3) What causes the persistent plasma emission (the M-region source) from activity centers?

SOLAR MAGNETISM

Although solar magnetism is known to be closely linked to solar activity, the relationship is poorly understood. Sunspots exhibit the strongest magnetic polarities on the surface. They seldom appear as simple dipoles or as the result of simple electric current systems. The elementary theory of magnetic diffusion suggests a natural sunspot lifetime of a few hundred years, in contrast to their observed lifetimes of a few weeks. Theories of the origin and dispersal of sunspot magnetic fields have to take into account

the resistance of the photospheric plasma to changes in magnetic fields. The usual explanations of rapid changes involve bulk transport of magnetized material by hydromagnetic processes. The microscopic relation of solar magnetism to velocity and thermal structure remains one of the most pressing observational tasks of solar astronomy. The scale of such correlative observations is limited by the resolution of ground telescopes to about one-tenth the otherwise attainable Doppler or direct resolution.

Important questions of immediate interest in solar magnetic observations concern magnetic properties of structures in the whole size range from a few hundred kilometers (prominence fibers, granules) through a few thousand kilometers (sunspots, prominence gross structure) to a few hundred thousand kilometers (global distribution of magnetic polarity and field strength). Many specific questions concerning solar magnetism remain unanswered, including the cause of north-south hemispheric spot polarity alternation and the alternation of leading-spot polarity between successive sunspot cycles. A theory of spot magnetism must account for the observation that some spots are bipolar, others predominantly unipolar, and others heterogeneous. Observations, rather than theory, will probably reveal how solar magnetism on the largest scale (general field) evolves in relation to the 11-year solar cycle. Related to this phenomenon is the enigmatic discovery that the magnetic fields at the Sun's N and S poles do not change polarity in phase with each other.

At the other end of the known size scale, it is not yet determined whether granules or chromospheric spicules are discretely magnetized. The relationship of their magnetic and geometric properties to their kinematic behavior is the cornerstone of any theory of these phenomena and probably of gross forms of solar activity as well.

Ultimately, we seek to learn the origin of the Sun's magnetic fields. Solar rotation and the convective transport of subphotospheric plasma have been suggested as the basic mechanism, but these theories cannot yet predict the observed character of magnetic fields in spots or the general field. In this general area of

research, exploratory observations will probably precede advances in theory for some time to come.

ATMOSPHERIC INHOMOGENEITIES AND TURBULENCE

At the limit of attainable ground resolution, photospheric granulation reveals the vital role played by turbulent convective energy transport in the steady-state configuration of the Sun. Higher in the atmosphere off-band hydrogen spectroheliograms disclose the vertical transition from microscopic turbulent energy transport to a larger scale process. The supergranulation has recently been discovered to be intermediate between these small scale motions and the grosser inhomogeneities of sunspots and activity centers. The relationship between the supergranulation, solar magnetism, and active centers is only known in a crude way and is not understood at all. All the most difficult tasks of solar observation are united in this area. Weak-field magnetometry of small structures, monochromatic time lapse pictures made simultaneously at several wavelengths, and velocity-discriminating observations must be made continuously over extended periods of time.

In the higher layers of the solar atmosphere, different characteristic inhomogeneities dominate. In the chromospheric transition layer, the spicules correspond to the small-scale turbulent velocity field surrounding active regions. During the last decade monochromators and high-resolution spectrographs were first applied effectively to study spicules at the limb. Quite recently, off-band techniques combined with time-lapse photography have provided meaningful new observations of spicules on the disk. The new data have not, however, answered the basic question of why spicules occur.

The corona has been shown at many total solar eclipses to have the shape of an oblate spheroid with discrete radial streamers. The size and distribution of coronal features vary with the solar cycle but also from day to day as the Sun rotates and as the individual activity centers evolve. Indirect evidence of inhomogeneities in the corona is provided by variations in the temperature of the solar wind. These variations have been observed directly by interplanetary space probes and inferred

from their effect upon the Earth's magnetic field. The mechanism of this influence is not understood.

More highly organized coronal forms are familiar as prominences and are readily visible as condensations of partially ionized gas having a variety of shapes. Most of the information about these forms is puzzling: why they form, how they can persist, their relation to activity centers in the chromosphere, details of their fine structure, and their passive response to chromospheric impulsive activity.

The forms and variations in coronal structures at the limb can be observed by combining the coronagraph with the birefringent filter. Satellites, however, will be required to study this form of solar structure in sufficient depth to understand it.

FLARE PHENOMENA

A flare is a localized, sudden brightening of the chromosphere in H-alpha or the calcium K-line. Large flares often produce associated radio noise bursts, sometimes cause sudden-commencement magnetic storms, usually produce flashes of X-rays, occasionally eject energetic protons, and (apparently fortuitously) disturb prominences in the neighboring corona. A vast amount of detail is known of these chromospheric brightenings, but as yet it can only be guessed how a flare is formed; why it occurs, where and when it does; or how it relates to the concomitant nonthermal phenomena. The answers to this particular set of questions continue to rank among the principal objectives of solar astronomers.

Numerous flare theories have been advanced during the past few years, some of which could possibly be tested by direct observation. Typical of these are theories postulating the transfer of magnetic energy to streams of charged particles by such plasma mechanisms as pinch discharges and the Fermi process. Observations made with unlimited wavelength, magnetographic, angular, and time resolution over the whole electromagnetic spectrum could conceivably test the validity of such theories. One goal of solar astronomy is to test such theories by following promising lines of specialized observations. A simple example is the theory of magnetic relaxation of the entire field of a sun-

spot group. This theory could be tested with magnetic maps, accurate to a few gauss and a few hundred kilometers, by comparing preflare with postflare sunspot configurations.

Familiar spectroscopic and cinematographic techniques will continue for a long time to play a major role in flare studies, especially as advances in technology or superior observation sites improve observational capability. For some questions, increasing the resolution in the visible spectrum could be as important as extending modest-resolution observations to an unexplored spectral region. In general, however, the greatest promise for understanding flares is offered by high angular resolution, and high time resolution X-ray and ultraviolet studies of the rising phases of flares, including the analysis of line profiles of critical emissions. This observational objective can be stated in terms of numerous specialized observations, of which the following are only typical: 5- and 1-arc-second resolution X-ray pictures of flares, both in resonance lines (such as Lyman-alpha of C VI or O VIII) and in the continuum near 1 Å and 10 Å; maps of the Sun's face showing the variation in the profile of the hydrogen Lyman-alpha line, especially the extended faint wings, with resolution of structures as small as 100 km; spectrograms in the entire extreme ultraviolet region (100 Å–3000 Å) of the hottest portions of flares, to obtain time variations of equivalent widths of multiplets over the range of excitation and ionization energies; and polarization observations of the continuum radiation emitted from flaring regions.

The radiofrequency emission of flares has been energetically investigated during the past solar cycle. Together with direct measurements of solar protons, this technique has revolutionized our outlook on flares, on the Sun, and even on the universe. Because wavelengths of a meter and more are involved, angular resolution is only adequate to locate radio bursts relative to activity centers. In theory, very large telescopes operating at centimeter wavelengths could provide detailed radio-emission maps of flares to show how their nonthermal and their quasi-thermal processes are associated geometrically. The basic physical mechanisms may be determined by polarization and spectral

analysis at high angular resolution for investigating local magnetic fields or for discriminating between basic radiative processes. At very long wavelengths, low spectral resolution observations alone may provide additional information on the origin of the radiofrequency emission.

RELATION BETWEEN GROUND AND SPACE OBSERVATIONS OF THE SUN

From ground observatories we see principally the quasi-thermal radiation of the Sun. The nonthermal emission, from which the desired information on solar activity could be obtained, lies near the threshold of detectability in the visible region. Only with the most refined monochromators, Hale's spectroheliograph and Lyot's birefringent filter, can this emission from the chromosphere and corona be measured, because the Sun's spectral luminosity reaches peak intensity near 5000 Å, right at the center of this atmospheric window. At the extremes of the electromagnetic spectrum, in the ultraviolet and radiofrequency regions, the quasi-blackbody radiation is much weaker than the nonthermal component.

Despite this handicap, observations from the ground must play a dominant role in solar research for many years to come. Angular resolution of a high order is required for studying such structures of solar activity as spots and flares and such inhomogeneities of the quiet Sun as spicules and granulation. The atmosphere permits apertures up to about 30 inches to be used. To achieve a resolution higher than about 0.3 arc-second, larger aperture telescopes must be carried above the atmosphere; this will be done by balloons and eventually by satellites. In the meantime, solar observations from space vehicles serve best in the inaccessible extreme spectral regions, using the modest angular resolution possible by the size of telescope and precision of stabilization available. Radio emission from the Sun offers a most powerful tool to discover and monitor nonequilibrium processes from the ground. However, high-enough angular resolution at centimeter, meter, and decameter wavelengths cannot be attained to investigate basic structures like spicules, prominences, spots, and granulation, because at such

wavelengths high-resolution telescopes grow to prohibitive dimensions.

In another way, satellite observations even today can, in principle, excel ground observations. Continuity of observation is essential to study adequately the rare and unpredictable solar events of greatest interest, such as flares. Our understanding of the supergranules is presently hampered by inadequate observations of their time development, as one observatory can follow the evolution of an element only throughout part of its lifetime during each day. Satellites carrying large telescopes in continuously sunlit orbits will eventually permit such studies to proceed over arbitrarily long times without interruption by sunsets and cloudy days.

Meantime, simple satellites permit uninterrupted monitoring of the X-ray brightness of the Sun and could, if desired, provide the equivalent of a chromospheric-flare patrol in hydrogen light. That function is currently performed more economically from the ground because no firm requirement exists for the guarantee of complete monitoring. If a few gaps in coverage, up to a few hours length can be tolerated, a relatively inexpensive H-alpha patrol network can replace a more expensive orbiting monitor. This situation may change as operations in space generate a firm requirement for reliable, full-time monitoring.

chapter 3

Instrumentation

SIGNIFICANT PROGRESS has been made in developing the tools of space solar astronomy. Since mere invention of a new technique often enables a number of new scientific advances to be made, we shall consider this technological progress in detail. This topic has been reviewed comprehensively in reference 1.

SOLAR POINTING CONTROLS

Early rocket flights were made without any attitude-control systems, and experimenters had to rely on the rocket's tumbling to sweep their detectors across the desired field of view, together with a Sun sensor to establish the detectors' attitude as a function of time. The NRL satellites SR I and SR III were also unstabilized and their detectors operated in a sky-sweeping mode.

In contrast, the present generation of satellites features many sophisticated attitude control systems (ref. 2). Before the introduction of reliable 3-axis attitude control systems, satellites such as the Explorer and Pioneer series successfully employed spin stabilization to achieve single-axis stability. This technique is still attractive, especially for equatorial or near-polar orbits where uncontrolled spin stabilization can be maintained for durations of 1 to 3 years.

Probably the most sophisticated active stabilization system to date is that used on OSO I, which is designed to point 75 pounds of instruments at the Sun with an accuracy of 1 arc-minute. In addition, 100 pounds of instruments are housed in a spinning section of the spacecraft and scan the Sun once every 2 seconds. Unlike passive systems, the spin rate on OSO I is maintained within 5 percent of its nominal value by small reaction jets, with a lifetime of at least 6 months. The spin axis itself is similarly maintained within 3° (ref. 3).

The Advanced Orbiting Solar Observatory (AOSO), successor to OSO, also will employ an accurate attitude control system which points the spacecraft at the Sun with an error of less than 5 arc-seconds, a vast improvement on the systems mentioned earlier. The AOSO system can also operate in a scan mode, producing a 60-line scan of a 5-arc-minute square positioned anywhere on command within a 40-arc-minute square centered on the Sun. In addition, a coarse scan of the whole 40-arc-minute square is possible; this function is also performed by the second and certain later OSO's.

The effect of such accurate pointing systems on the scope and design of solar experiments is not hard to see. While experimenters once had to be content with fleeting looks at some unspecified part of the solar disk, they can now design experiments to scan accurately specific areas of the Sun and observe time-variant phenomena with the assurance that it is the phenomenon that is changing and not the direction in which their equipment is being pointed.

DETECTORS

Soft X-Rays (1 Å—100 Å)

The fact that most materials in the soft X-ray region are highly opaque is a serious limiting factor in detection. Ionization type detectors with extremely thin windows are commonly used; photographic emulsions are also suitable. Scintillation counters and devices using phosphors or semiconductors are generally suitable for the hard X-ray, ultraviolet, and longer wavelength regions; however, they are inefficient in the soft X-ray region because the X-rays are absorbed in the top few microns of the detector surface. Photoelectric devices work satisfactorily, although with lower efficiencies than in the ultraviolet and visible regions. The X-rays penetrate the surface sufficiently for some of the photoelectrons to be captured before emission.

Photographic Emulsions

The first detector used for solar soft X-rays was photographic emulsion, with a thin shield of beryllium foil to mask visible

and ultraviolet radiation (ref. 4). Photographic emulsions have been used as detectors in pinhole cameras (ref. 5), and in photometers (refs. 6 and 7). In the soft X-ray region a linear relation exists between exposure and film density at low film density, and emulsions have been used for absolute calibration (ref. 8). The sensitivity of emulsions to X-rays is quite high, approaching 1 developable grain per photon.

Photoionization Detectors

Photoionization may be used to detect soft X-rays in ionization chambers, Geiger counters or proportional counters. The ionization counter is least sensitive and is used in very high flux conditions (refs. 9, 10, and 11) and is commonly filled with argon or nitrogen. Geiger counters will count single photons and are simple and robust; they have been used for a number of rocket and satellite observations (refs. 9 and 12).

The counter developed by NRL for solar soft X-ray work is described by Newell (ref. 13). Proportional counters will also work satisfactorily in the soft X-ray region up to about 20 Å and give moderate wavelength resolution by pulse-height analysis. Stable gas fillings and high voltages are required to obtain constant and reproducible response. Proportional counters have been developed at the University of Leicester (ref. 7) and have been flown on Skylark rockets (ref. 14) and on Ariel I (ref. 15). Typically the counters use a mixture of argon and methane at a pressure slightly less than 1 atmosphere. The methane acts as a quenching agent at high counting rates. Ionization detectors are the most common in solar soft X-ray rocket and satellite experiments conducted so far and will also be included on most of the OSO series of satellites. Typical spectral responses are shown in figure 1.

The performance of ionization counters is considerably affected by the absorption of the window. Only elements of low atomic number can be present in the window because they have the least absorption; typical window materials are beryllium, aluminum, mica, and plastic films such as Mylar, Glyptal, and nitrocellulose. The absorption is strongly wavelength dependent, especially if absorption edges are present in the soft X-ray

region. Extremely thin windows are required, of the order of a few microns thick; or for wavelengths of 50 Å, of less than 1 micron. This requirement presents some technical problems which have been solved by using small-area windows, by supporting the thin film on wire mesh, and by using flow counters to eliminate the effects of pinholes and leaks.

Window absorption usually determines the long wavelength limit in photographic detectors and ionization counters; in some cases it can be used intentionally to limit the response. The use of multiple filters with an absorption edge in the required wavelength range (as is the case with aluminum) enables a narrow band to be isolated, but this technique is limited to a few bands by the characteristics of available materials.

Photoelectric Detectors

In the soft X-ray region the quantum energy is high enough to eject photoelectrons from most solid materials. As noted earlier, however, the photoelectric efficiencies of common

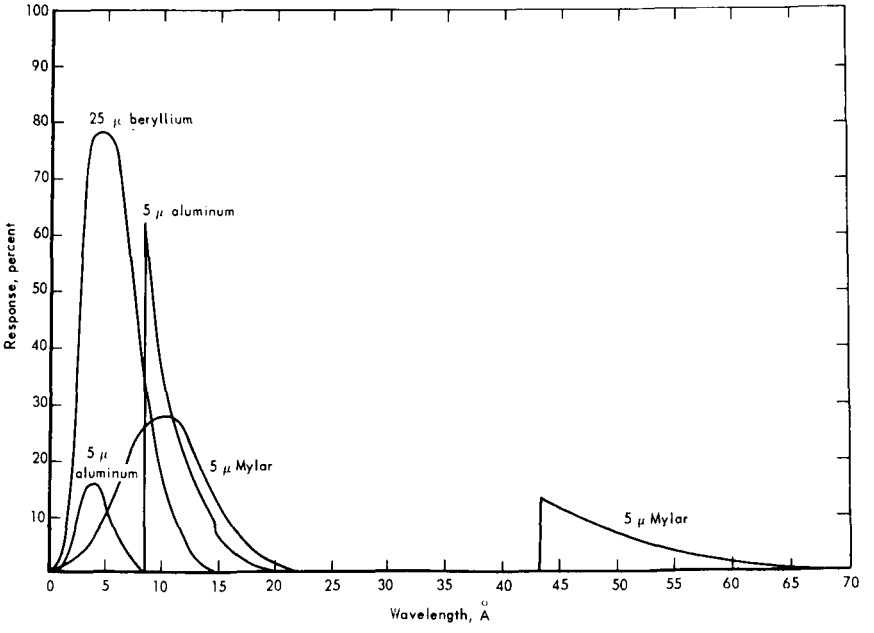

Figure 1.—Typical spectral response of ionization counters. Window material and thickness are indicated on the curves.

photocathode materials are generally lower than in the ultraviolet or visible, but a number of unconventional cathode materials such as beryllium, tungsten, and titanium show an appreciable effect with soft X-rays and negligible emission in the visible and ultraviolet (ref. 16). Detectors using these cathode materials, while having counting efficiencies less than Geiger or proportional counters, can be used without windows in the space environment. Photoelectric detectors for soft X-rays are usually open-ended photomultipliers, and since a volume rather than a surface photoelectric effect is involved, the cathode surfaces are less affected by exposure to the atmosphere than are conventional materials. Photocathodes of BeO and SrF_2, have been used in Russian detectors (ref. 17). Investigation of the possibility of using transmission photocathodes to make soft X-ray image converters and dissectors is included in the OSO and AOSO programs.

Scintillation Counters

Scintillation counters with beryllium or aluminum windows and NaI-Tl crystals have a response from 20 to 200 keV (10 keV=1.25 Å), beyond the short wavelength limit of the soft X-ray spectrum. With pulse-height analysis they can be used to map the spectrum above 20 keV in a similar manner to the proportional counter.

Most soft X-ray detectors are also sensitive to the charged particles in the radiation belts and in the solar wind. The low energy particles are stopped by the windows if present, while those of higher energy are usually deflected from the window aperture by "broom" magnets. Even this arrangement may be insufficient for particles of very high energy, and it is usual in these cases to use either closed counters or special cosmic ray detectors with anticoincidence techniques. In most cases, regions of high particle flux can be avoided by suitable choice of orbit. In the case of OSO I the energetic electron flux is avoided by the nearly circular, 300-nautical-mile-high orbit, inclined at 30°. However, the regions of higher flux (e.g., in the South Atlantic anomaly) are not completely avoided. Conversely, high

inclination orbits will suffer most from transit of the trapped radiation belt at high latitudes.

Ultraviolet

Photocells

For many years the only spectrally selective ultraviolet detectors had been the pure metal type which resulted from the early work of Rentschler et al. (ref. 18). Typical of these metals are gold and nickel, with gold having better rejection at longer wavelengths. Another useful material is the composite surface cesium-antimony, although the extension of its usefulness into the vacuum ultraviolet has been slow. Over a period of some 15 years, however, it has been possible to extend the range of such surfaces to nearly 1000 Å by the use of various windows. Dunkelman (ref. 19) describes this progress and has obtained a flat, high efficiency ($>10^{-1}$ photoelectrons/quantum) down to 1200 Å for a Cs-Sb photomultiplier using a CaF_2 window. LiF windows have extended the sensitivity to nearly 1050 Å.

A more significant advance in ultraviolet detection occurred when several akali-tellurium surfaces were developed by Taft and Apker (ref. 20). Since then numerous other workers have prepared both opaque and transparent alkali telluride surfaces, with some of the opaque surfaces having a quantum efficiency near 50 percent at 2500 Å. Notable among these are Cs-Te and Rb-Te, which have nearly the same efficiencies and rejection ratios. The alkali tellurides have a high work function and are particularly useful in applications where discrimination against longer wavelengths is important. Other materials with still higher work functions which are spectrally selective for the vacuum ultraviolet region are certain iodides and bromides; these substances are deposited on a thin conducting substrate of tungsten behind a LiF window. Typical for these detectors is a peak yield between 10^{-2} and unity near 1000 Å and a cutoff between 2300 Å and 2500 Å. In general, then, with suitable windows, certain cathodes provide satisfactory yields to approximately 1000 Å, with sharp cutoff or wider spectral response available as desired.

Another recent, significant development is the windowless continuous-channel multiplier designed by Goodrich and Wiley (ref. 21) which, because of its tiny size and high sensitivity, is unique among photocells. This multiplier is simply a short glass tube with its internal wall coated with a high-resistance layer. A potential difference of 1000 to 2000 volts is maintained between the ends, resulting in a current on the inner surface and a uniform axial electric field down the length of the tube. A photoelectron ejected from the inner surface near the open end is accelerated down the channel by the high voltage; multiplication occurs at each collision with the wall. The emitted electrons cascade down the length of the tube, producing gains of 10^5 or more.

A rather recent study of this multiplier (ref. 22) has shown it to have a spectral response similar to that of tungsten, although the photoemitting inner surface is an oxide of some other metal. Thus it is perfectly suited to measurements in the extreme ultraviolet, since it is insensitive to strong, near-ultraviolet and visible radiation which appear as stray light in any spectrum produced by a single grating.

Goodrich and Wiley (ref. 23) also developed another type of tube which was modified in collaboration with Hinteregger for the rocket-borne grazing incidence measurements. This is a magnetically focused, strip-type photomultiplier, with multiplication gain produced through crossed magnetic and electric fields. Photoelectrons, after emission from the cathode, move into the space between the two resistance strips where they follow a trochoidal path down the corridor between the strips, producing many secondary electrons at each collision with the secondary emitting surface. A gain of 10^8 or more is achieved. This type of phototube has been used successfully in the range of 55 Å to 1300 Å.

Uvicon

The uvicon is an ultraviolet-sensitive image tube, the main components of which are a photocathode, an electron imaging section, an electron-bombardment-induced-conductivity (EBIC) target, and a standard vidicon gun. The photocathode

assembly may consist of a LiF lens, a semitransparent conductor and a photoemitting material. The electrons released from the photocathode are electrostatically accelerated and focused on the EBIC target by a multielectrode system. The image size and focusing may be controlled by lens-element voltage ratios.

Energetic electrons released from the photocathode strike the target and generate a video signal. Each electron incident on the target generates charge carriers whose number depends on the voltage across the target material, the energy of the incident electrons, the temperature of the target material, and the composition. One such tube, designed for astrophysical purposes (ref. 24) had a gain of 500 for 40 volts on an arsenic trisulfide target.

After this tube was evaluated for use in Project Celescope, certain changes were made until finally a transmission-secondary emission target was employed. With this target, the minimum detectable point image (i.e., the image for which peak signal equals rms noise) contains about 1.4×10^3 photoelectrons. This value refers to measurements conducted at 30 frames/sec, 4 Mc/sec video bandwidth, with laboratory equipment. The uvicon and related detectors have not yet been employed to observe the Sun. These devices offer a most promising new technique to increase the data-acquisition rate of planned satellite experiments.

IMAGE SYSTEMS

Soft X-Rays

The soft X-radiation flux from different parts of the solar surface varies considerably. Therefore, it is important to make spatially resolved measurements of the X-ray flux so that a complete intensity pattern over the whole surface can be obtained at any instant of time. Problems of angular resolution, solar flux levels, and detector area limit the system performance; but considerable effort is presently being put into this field, and it forms an important part of the OSO program.

The refractive index of soft X-rays in all familiar materials is less than unity, and they are easily absorbed so that conventional mirror and lens imaging systems cannot be used. Reflection coefficients for soft X-rays are negligibly small except

at grazing incidence angles of less than 1°. Imaging systems of three kinds are possible—pinholes, zone plates, and reflection optics used at grazing incidence.

A pinhole camera with filters and photographic emulsion was used to obtain the first soft X-ray photographs of the Sun (ref. 25) and later photographs were taken by the Leicester group. Fresnel zone plates have been suggested for use in the soft X-ray region (refs. 26 and 27) but are extremely small and difficult to make and are nonachromatic. Their advantage over the pinhole for soft X-rays is a shorter telescope length, but potentially they are of greater use in the ultraviolet.

The technology of reflection optics for soft X-rays is still in its infancy. Reflection is fairly high for a number of materials for grazing incidence angles of less than 1° (ref. 28). Such reflectors are usually tubular, the mirror profile being accurately machined on the inside of the tube. Various surface shapes have been considered, but single-reflection surfaces have severe astigmatism and are only suitable as collimated light gatherers when used with a limiting aperture. Some double-reflection profiles are stigmatic and form good X-ray images over small collection angles. An X-ray telescope was proposed by Giacconi et al. (ref. 29), and is shown in figure 2. This field is being studied extensively by NASA (ref. 30). X-ray reflection telescopes of both the collimating and image forming types feature prominently in the OSO and AOSO programs.

Mechanical collimation systems can also be used with soft X-rays, but they require scanning to build up a complete X-ray picture and are, therefore, more suitable for satellite than rocket vehicles. To obtain high sensitivity, multiple collimation apertures are required, together with large-area detectors. In principle, their mechanical simplicity enables them to compete with the more complex reflection telescopes, but the latter are already being developed greatly.

Ultraviolet

Since astrophysical studies in the vacuum ultraviolet can now be carried on from outside the atmosphere, it is of interest to consider the possibility of obtaining solar images in this spec-

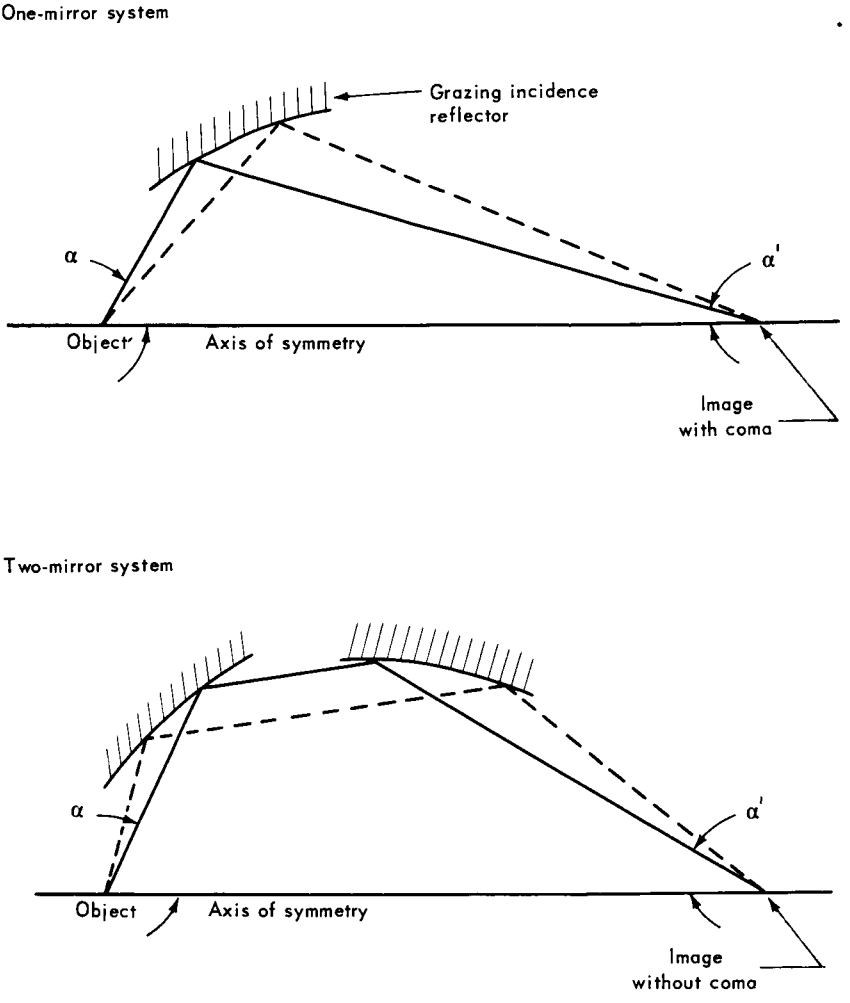

Figure 2.—**Optics for grazing-incidence X-ray telescope.**

tral region, suitable for television transmission. To form the first optical image at the camera tube in the vacuum ultraviolet, the radiation should not traverse an absorbing medium. In addition, it is desirable to image selectively within the camera tube's sensitive range. Thus a possibility for a suitable optical system is a zone plate constructed without a substrate (ref. 31).

Such a zone plate has been investigated by Baez (ref. 26) for application to visible and ultraviolet image formation. It consists of an array of concentric rings which are alternately

transparent and opaque. The radii of the ring boundaries increase as the square root of successive integers. At a distance from the zone plate proportional to the square of the outside radius of the largest transparent ring, and inversely proportional to the illumination wavelength, light from every other half-period zone is blocked off, so that all arriving light is in phase and self-reinforced. This position is the primary focus.

The first plate consisted of a set of thin circular gold bands made self-supporting by radial struts, leaving the transparent zones empty. The diameter was 0.26 centimeter and it contained 19 opaque zones, the narrowest of which was about 20 μ across. Tests were made in visible light and in the ultraviolet only as far as 2537 Å. Resolution and speed of the zone plate are greatly improved over the pinhole. The plate compares favorably in resolution, but not in speed, with a simple lens, if comparison is made in the visible region. Below 1000 Å, however, the speed is millions of times greater than that of a lens made of any known material. The zone plate promises to be a useful focusing device for the extreme ultraviolet since the reflectivity and transmissivity of known materials makes lenses or mirrors extremely inefficient in this region.

SPECTROMETERS

Soft X-Rays

In the soft X-ray region, wavelength resolution can be obtained as follows:

(1) By selective absorption in a filter composed of one or more selected materials or by selective response in the detector
(2) By proportional counters with pulse-height analysis
(3) By Bragg reflection from a crystal, either flat or curved

While the grazing incidence spectrograph can resolve wavelengths well down into the soft X-ray region, it is currently used primarily in the vacuum ultraviolet region and will be considered in that section.

Selective Absorption

Selective absorption occurs in detectors and windows, either intentionally or otherwise, and in many cases is used intentionally to obtain wavelength discrimination. The first wavelength-resolved measurements of solar X-rays were made by NRL with rockets. By using beryllium, aluminum, and Mylar windows (ref. 9), counters have been made sensitive to the wavelength regions 1 Å–8 Å, 8 Å–20 Å and 44 Å–60 Å, respectively (see also fig. 1). The use of composite windows and comparison of the signals from counters with different windows enable smaller wavelength regions to be isolated, and the use of selected counter gases such as argon (which has a K edge near 4 Å) can give a selective response. These wavelength bands are broader, however, than is desirable and cannot be refined sufficiently. Also, the rapid variation of sensitivity over the passband of the composite filters and detectors makes interpretation of results difficult.

During the early pioneer work in the solar soft X-ray field and during subsequent work up to 1962, this type of detector has provided most of the existing information on the solar spectrum distribution. An indirect method of obtaining wavelength resolution has been used by the NRL group (ref. 32) and a Russian group (ref. 33) on rocket flights. This technique relies on the selective absorption of the atmosphere over the rocket trajectory; the harder X-rays penetrate to the lower altitudes, while the softer components increase in intensity with altitude. Hinteregger has employed the same effect to analyze the composition and structure of the upper atmosphere.

Proportional Counters

Using photoionization counters in the proportional region considerably improves the wavelength resolution. High resolution can be obtained at the short wavelength end of the X-ray spectrum, but at wavelengths greater than 20 Å too few ion-pairs are produced to obtain satisfactory resolution. Hence these counters have been used primarily to map the short wavelength end of the spectrum and cannot be used to detect

or identify line spectra. Much development work on soft X-ray proportional counters has been done by groups at Leicester and London Universities. They have been flown on Skylark rockets and on the Ariel I satellite (ref. 15) and feature prominently in the OSO program.

Bragg Crystal Spectrometers

The crystal spectrometer is similar to that used for hard X-rays (using a reflection crystal set at the "Bragg angle"), but it uses crystals with relatively large lattice spacings of the order of 10 Å. They have high resolution, comparable to that of grating spectrometers in the ultraviolet and will resolve emission-line spectra. Such spectrometers (actually, scanning monochromators) have already been used to observe soft X-rays from laboratory plasmas (ref. 34) but have only recently been developed for solar observations. The reflection coefficient of the crystals is usually small for soft X-rays, and a high degree of collimation is necessary to obtain good spatial and wavelength resolution. Certain organic crystals such as potassium hydrogen phthalate enable measurements to be made to 25 Å and combine a reasonable reflection coefficient with a uniform crystal structure. As this particular field is in its infancy and considerable importance is attached to wavelength resolution, much effort is being currently applied to advance the technology.

A Bragg crystal spectrometer has been developed at NRL and flown on an Aerobee rocket. This and a spectrometer developed by NASA (ref. 35) will be flown on OSO satellites. The NASA 1–400-Å spectrometer developed by Goddard Space Flight Center actually consists of three separate Bragg crystal monochromators and an ultraviolet grating spectrometer. The crystal monochromators cover the ranges 1–3.8 Å, 3.6–8.4 Å, and 8.2–25 Å. Parts of this instrument are shown in figure 3. The detectors for the first two ranges are ionization counters while the third is a Bendix open photomultiplier.

Future efforts in the crystal spectrometer field include extension of the technique to longer wavelengths, up to about 100 Å,

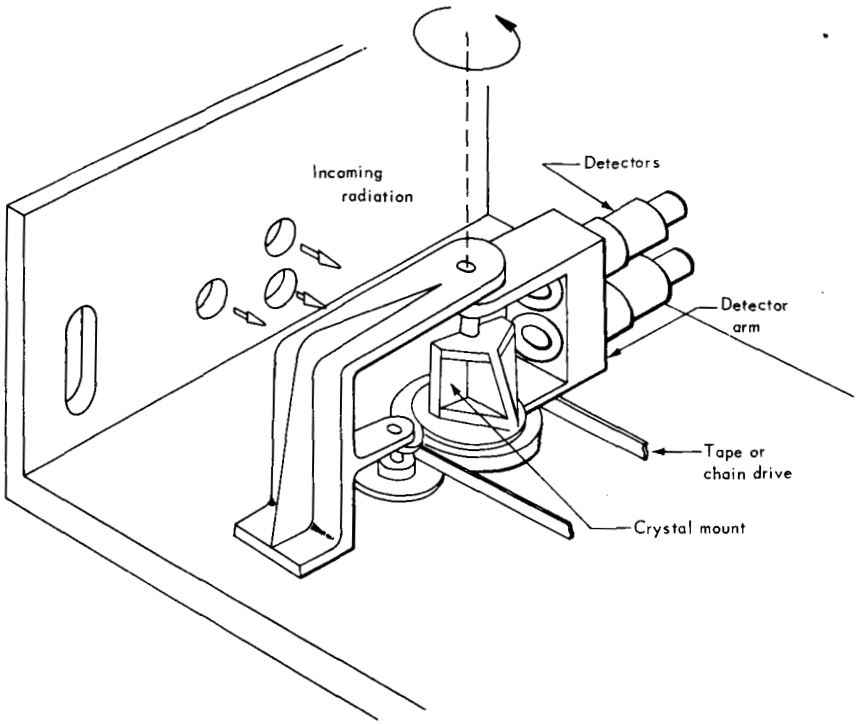

Figure 3.—Crystal spectrometer for 1 Å–8.5 Å.

thus insuring complete overlap with grazing incidence spectrometers. For this purpose the development of crystals having large lattice spacing is being studied.

Bent-crystal spectrographs, analogous to conventional Rowland-circle spectrographs in the visible and ultraviolet, offer the possibility of improved light collecting efficiency over the monochromator. They have been employed recently on rocket flights using photographic film to record the dispersed spectra, but they will require the development of X-ray image converters for use on unmanned satellites.

Recently (1964) the Los Alamos group (H. V. Argo, J. A. Bergey, W. D. Evans, B. L. Henke, and M. D. Montgomery) have developed and flown bent-crystal monochromators on Nike-Tomahawk rockets. The equipment had a pointing accuracy of about $2\frac{1}{2}°$. A series of fixed-wavelength monochromators were flown using crystals of mica and films of organic

materials including lead stearate. Resonance lines such as C V, C VI, N VI, N VII, O VII, and O VIII in the wavelength range 16–40 Å were isolated and detected by thin-window gas-flow Geiger counters.

Ultraviolet

Normal Incidence Wavelength Region

All spectrographs designed for rocket flight have used a reflection-type diffraction grating as the dispersing element. Because of the interest in the extreme ultraviolet spectrum, lenses have generally not been employed, and focusing is by reflection only.

Work with such instruments began in 1946, but it was not until the very active period during the 1950's that most advances were made. A number of instruments were designed and flown during these years; however, the stray light produced by the intense long-wavelength portion of the solar spectrum always set a detection limit on the weak emission lines in the extreme ultraviolet. Improved measurements have been made more recently and are described in a review by Tousey (ref. 36). The first good results were obtained with the 1959 flight of Purcell, Packer, and Tousey (ref. 37) which succeeded in showing a number of lines in the Lyman series of hydrogen and the Lyman continuum. The photospheric continuum was also detectable to approximately 1700 Å, below which it was swamped by instrumental stray light. These results were recognized as being about the best that could be obtained with a single-dispersion system.

The greatest improvement in the normal-incidence spectrograph was achieved with the doubly dispersing instrument of Detwiler et al. (ref. 38) shown in figure 4. The new spectrograph was essentially the normal incidence instrument used in previous NRL experiments, with an added predisperser grating, external to the slit, instead of a collecting mirror. The predisperser grating is of 40-centimeter radius of curvature, having 600 lines/mm. The dispersion is arranged to be along the slit; thus the visible and near ultraviolet portions of the

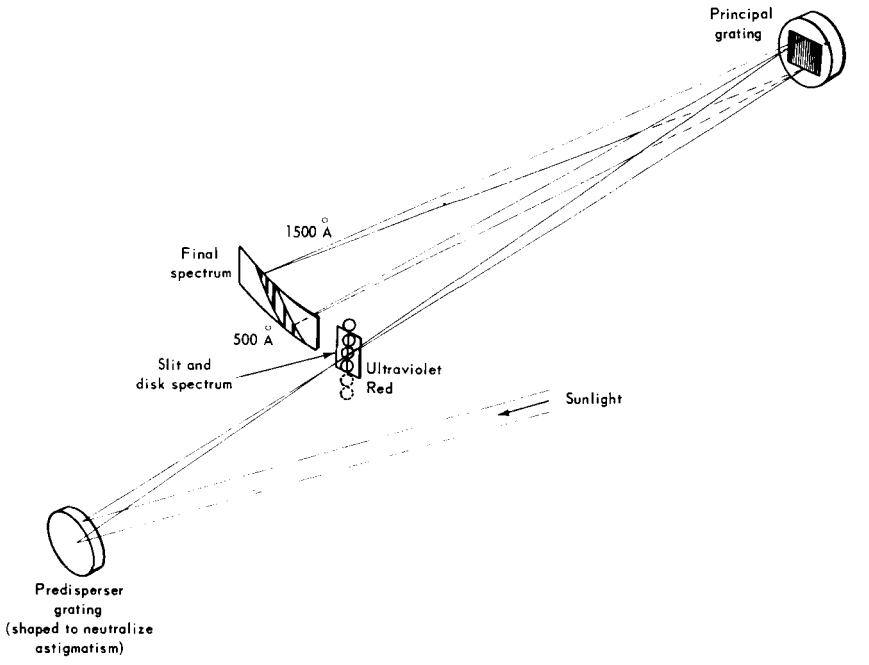

Figure 4.—**The double-dispersion spectrograph (ref. 38).**

spectrum fall beyond the slit and do not enter the spectrograph. The dispersion directions of the two gratings are at right angles so that the final spectrum is tilted, causing only a slight difficulty in using a densitometer.

The double-dispersion instrument was used first in April 1960, and twice again in 1962. Resolution of 0.1 Å was obtained in one case. Because of the nearly complete elimination of stray light, it was possible to follow the continuum down to nearly 800 Å. In addition, many lines previously unresolved were separated and some profiles measured.

Grazing Incidence Wavelength Region

For many years it has been known that wavelengths near 100 Å or less can be resolved with diffraction gratings using near-grazing incidence. The first solar spectrograph using a grazing-incidence grating was flown in 1952 by Rense (ref. 39). Several improvements were then made and in a 1959 flight the instrument was successful in detecting for the first time the resonance

line of He II at 303.7 Å (ref. 40). Because of the high level of stray light, however, the spectra were difficult to interpret.

Another instrument, designed at NRL by Austin, Purcell, and Tousey (ref. 41) and flown in 1961 and 1962, used a 40-centimeter radius, 600 line/mm grating at 5° from grazing incidence. A 1000-Å-thick aluminum film at the entrance slit eliminated all stray light down to 830 Å. The region from 170 Å to 310 Å was transmitted well, however. During a 1963 flight, records were obtained clearly showing approximately 125 lines in this spectral region, with definition sufficiently sharp to permit determining wavelengths to 0.05 Å or better. Additional lines and some diffuse emissions were apparent as far down as 45 Å.

A different approach to grazing-incidence solar spectroscopy, using photoelectric recording and telemetry of data, has been followed by Hinteregger (ref. 42). The instrument shown in figure 5 uses a grating of 2 meters radius of curvature at 4° from grazing incidence. The detector is a Bendix magnetically focused strip-type photomultiplier (ref. 23) with a tungsten cathode, so that stray light of long wavelength has no effect. Photon counting rates from a maximum of some 10^6 per second down to about 20 per second are possible. During two 1963 flights, by reducing the spectral scan rate to 2 Å/sec and using a LiF photocathode, far fainter lines were detected than previously. It was also possible to reduce the slit width for these flights, so that the instrumental profile varied from 0.7 Å full-width at half-maximum at 315 Å to 0.35 Å at 55 Å. Lines were detected down to 65 Å.

High Resolving Power Spectrographs

Determining the true profile of a spectral line requires a resolving power of 10^5 to 10^6. To approach this with instruments designed for flight, high orders of interference must be used.

Figure 6 shows a normal-incidence instrument (ref. 43) using the 13th order, designed to obtain the profile of the hydrogen Lyman-alpha line. Both gratings have a radius of curvature of 50 centimeters and are ruled with 1200 lines per mm, providing a

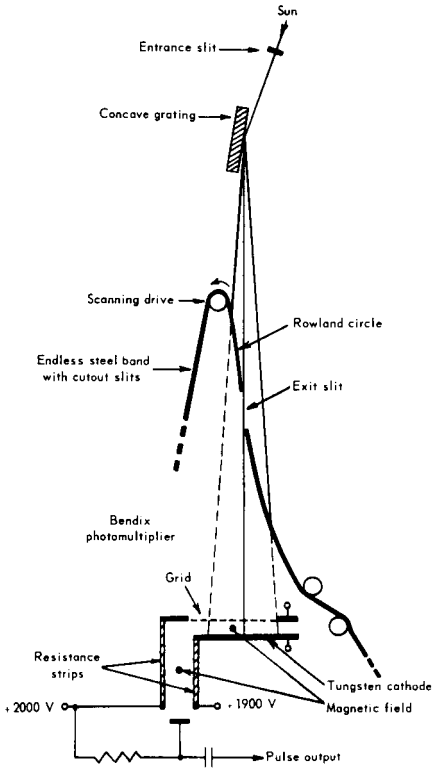

Figure 5.—The AFCRL grazing-incidence scanning monochromator.

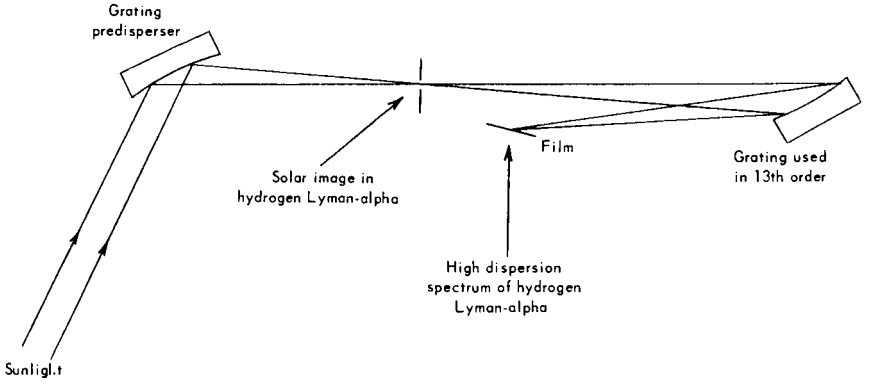

Figure 6.—NRL's stigmatic high-resolution Lyman-alpha line spectrograph.

dispersion of 0.4 Å/mm. Theoretically the instrument has a resolving power of 250 000. In practice, however, the resolving power is limited to 40 000 by the slit width, which was equivalent to an instrumental width of 0.03 Å. During two flights, excellent line images were obtained, from which it was possible to derive the emission line profile, as produced in the Sun and also as modified by absorption in the Earth's atmosphere.

To obtain extreme resolution in the range of 3000 Å to 2000 Å, the spectrograph shown in figure 7 was built at NRL using transmission optics. The echelle, with 73 lines/mm, pro-

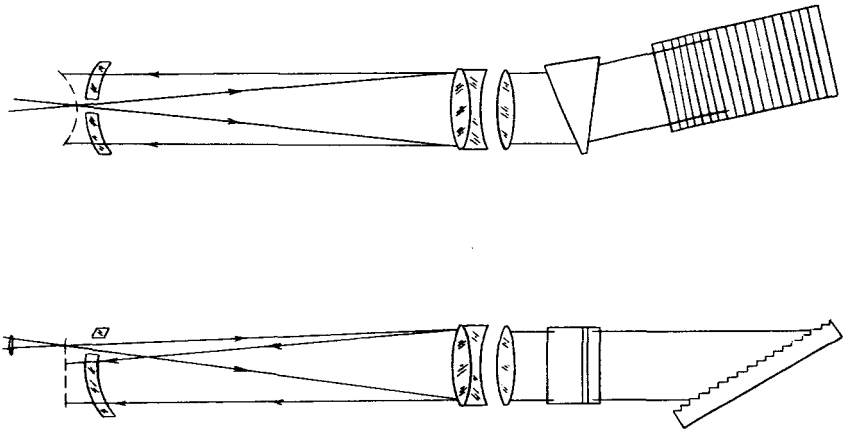

Figure 7.—**The echelle spectrograph for the 3000-Å–2000-Å range.**

duces a high dispersion at right angles to its rulings, in orders between 120 and 60. The dispersion produced by this instrument varied between 1.5 Å/mm at 3000 Å to 1 Å/mm at 2000 Å. Because of the stray light problem, a small monochromator was used as a predisperser. Generally, the instrument performed very well and produced spectra having approximately the same resolution as is attained with a 21-foot grating spectrograph. McAllister has developed an echelle spectrograph based on this principle for rocket observations of the Sun.

Another echelle instrument designed primarily for extreme ultraviolet radiation is shown in figure 8. This was constructed

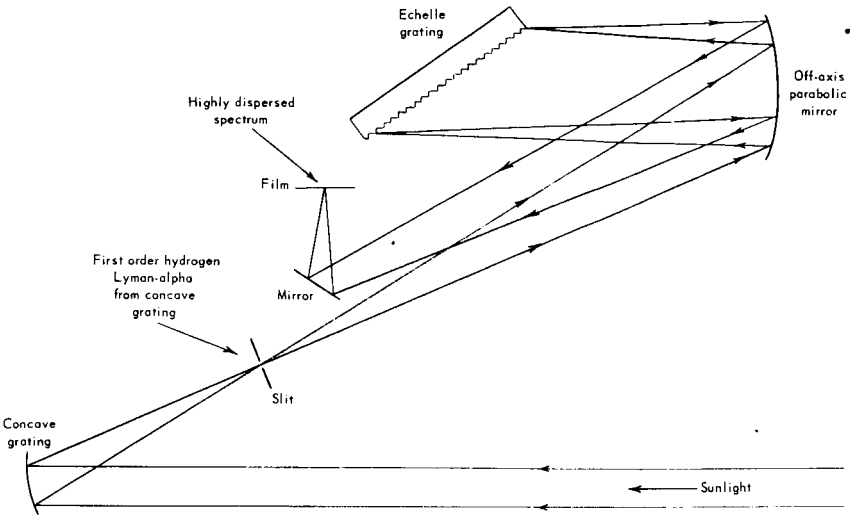

Figure 8.—**An extreme ultraviolet echelle spectrograph for hydrogen Lyman-alpha line.**

(ref. 44) using only reflecting optics and was intended for the hydrogen Lyman-alpha line. Only a few narrow spectral ranges could be covered, each approximately 4 Å wide. In the laboratory the instrument was adjusted for a resolving power of 0.007 Å. The first flight in 1961 failed because of pointing difficulties.

Chapter 4

Mapping the Sun's Ultraviolet Spectrum

NORMAL-INCIDENCE SPECTRAL REGION

IN TWO RECENT REVIEWS, Tousey (ref. 45) and Allen (ref. 46) describe certain features of the solar spectrum and this information's contribution to an understanding of solar physics. They also point out that the study of short-wavelength radiation has just begun and that many, more precise observations are required.

Within the 3000-Å to 2085-Å range, the Sun's spectrum is, as at longer wavelengths, a continuum with Fraunhofer lines. More than 6400 lines have been observed, although at least half of them cannot be identified from the multiplet tables. At present, only a small fraction of the data from this region has been published. The lines of greatest interest here are the H and K lines of Mg II, at 2802.698 Å and 2795.523 Å respectively, which produce a deep depression in the spectrum extending 20 Å or more to either side of their centers. The continuum level is also of great interest, although earlier results showed no regions between 3000 Å and 2085 Å where the true continuum could be seen. With spectra of 0.15-Å resolution, several places between 2641 Å and 2700 Å were reported where the continuum seems to be free from absorption and lies near the 5900° K level. Echelle spectra support this, but at shorter wavelengths there appear to be no windows through which the continuum can be seen.

Between 2100 Å and 2000 Å, a sudden change takes place in the spectrum. The intensity of the maxima between Fraunhofer lines falls sharply, and below 2085 Å it follows a 5000° K curve; this is a decrease by a factor of nearly 4 in less than 25 Å. However, no abrupt change occurs in the bottom of the lines, which continue to follow a 4900° K curve. The appearance is

one of blanketing by continuous absorption. The continuum is depressed, as though optical depth unity lay farther out in the photosphere where the temperature is 5000° K. Furthermore, the cores of the Fraunhofer lines seem to be formed at a higher level where the temperature is lower.

The radiation in the 2000-Å to 1200-Å spectral range represents the transition region between the photosphere and the chromosphere. The gradual transition from Fraunhofer spectrum to emission line spectrum takes place in this range so that no Fraunhofer lines can be seen below 1530 Å. Generally, the region between 500 Å and 1500 Å is represented by a continuum and emission lines, both of which originate in the chromosphere. The continuum is smooth except near hydrogen Lyman-alpha, where it builds up toward the line center from both sides. The most prominent emission lines in this region are those of the Lyman series of hydrogen. The other lines are primarily those of the more abundant light elements: He, C, N, O, Ne, Al, Si, and S. Most states of ionization, from neutral to 11 times ionized, are represented. Agreement between photographic and photoelectric data in this spectral region is excellent. Fluctuation in the photoelectric measurements is regarded as noise and does not generally interfere with line identification. A problem inherent in the photoelectric technique is, of course, that scanning reduces the amount of energy available in a given time so that it is difficult to obtain resolution as good as that of photographic measurements for the same experimental conditions. Photography is therefore expected to be of continuing value.

A brief review of the most significant flights has been given recently by Hinteregger (ref. 47). The first photographic evidence of some important lines in the extreme ultraviolet was obtained from University of Colorado flights in 1958 and 1959. Identification was difficult, however, because of a rather high background of stray light and certain film defects. The published list of observed wavelengths (ref. 40) attracted much attention, but it also led to considerable controversy, which was subsequently resolved by data from later flights.

The 1959 normal-incidence measurements made by NRL (ref. 37) apparently realized the full potential of the single-

dispersion photographic system. The photospheric continuum appeared detectable down to about 1700 Å, below which it became swamped by instrumental stray light. Many emission lines and a number of the hydrogen Lyman series were clearly recorded in these spectra, however. The data provided the first record of coronal emission of Ne VIII at 770 Å and 780 Å, as well as resonance lines of He I, N I, N II, N III, O II, O III, O IV, O V, Mg X, and S VI. The first indication of the hydrogen Lyman continuum was also observed.

The most notable step in reducing the stray light problem was taken with the introduction of the double-dispersion normal-incidence spectrograph by Detwiler, Purcell, and Tousey (ref. 38) which was flown in 1960 and again in 1962. Spectra obtained in 1960 covered the range from 1550 Å to about 500 Å with a dispersion of 41 Å per mm. Spectra with a dispersion of 20 Å per mm for the 2000–1200-Å region and 10 Å per mm for the 1250–800-Å region were obtained with two similar instruments in 1962.

Most of the emission lines in this region are chromospheric. For example, the first 13 lines of the Lyman series of hydrogen were resolved in the 1960 spectrum, and were followed by the Lyman continuum, with radiation temperature approximately 6650° K. He I and He II were noted, and the spectrum of C I was present with great intensity and completeness. Further details of these spectra are given in the review paper by Tousey (ref. 45).

The AFCRL telemetering monochromators were flown several times during the period 1959–61, producing a fair number of records from 1300 Å to 250 Å (ref. 48). Various emission lines were identified in this range and certain conclusions drawn from the spectra, particularly that obtained on the August 1961 flight. Among other things, the absence of lines from intermediate stages of ionization indicated that the transition between the chromosphere and corona is extremely sharp. It was also inferred that the chromospheric lines (corresponding to ionization potentials less than 100 eV) are emitted in a region of temperature less than 60 000 °K, so that the higher series members are weak. It

further appeared that ionization equilibrium in the corona is not much different from what had been expected.

The best resolution of the solar spectra was obtained in the range 3500 Å to 2200 Å with the echelle spectrograph of Purcell, Garrett, and Tousey (ref. 49) flown in 1961. A resolution of up to 0.030 Å was obtained, from the 81st order at 3000 Å to the 122d order at 2000 Å. Orders were separated by crossing the echelle with a CaF_2 prism. The spectra from 3500 Å to 2988 Å were of the same quality as spectra obtained from the ground by conventional astronomical techniques. From 3330 Å to 3350 Å, the echelle spectra agreed closely with the atlas compiled by Bruckner at Göttingen. Within the 2988-Å to 2200-Å range, the spectra contained some 4000 Fraunhofer lines. Wavelengths were established to approximately 0.010 Å by reference to the many easily identified lines of Fe I, Fe II, and other metals.

GRAZING-INCIDENCE SPECTRAL REGION

The first grazing-incidence data were obtained within the early series of AFCRL telemetering monochromator flights during the period 1959–61. The flights of January 1960 and August 1960 (ref. 42), using a continuously moving exit slit and signals of the position of the slit along the Rowland circle, yielded photoelectric data down to 60 Å. The monochromators were operated with a fast wavelength scan, resulting in a special resolution lower than might be expected. These spectra are largely of historical interest since they have been superseded by improved data. They did, however, illustrate a conspicuous dropoff of spectral intensities below 170 Å, leading to controversy as to whether this was a real characteristic of the extreme ultraviolet spectrum or an instrumental effect.

These data were compared shortly thereafter with NRL photographic records obtained with a grazing-incidence spectrograph during June 1961 and August 1962 (ref. 41). The wavelength coverage of these flights was from 700 Å to approximately 170 Å in first order. The lower cutoff was caused by an aluminum filter which was used to suppress stray light and which became extremely opaque at this point; however, had shorter wave-

lengths been present with great intensity they might have been recorded in second order. Since this was not the case, the earlier discovered dropoff below 170 Å was neither really confirmed nor contradicted. Above 170 Å the agreement between the photoelectric and photographic records is entirely satisfactory. About 50 solar emission lines were observed with wavelength precision of 0.1 Å, by using He II 303.78 Å as standard. The most interesting of the identified lines were those of C VI at 182.35 Å and Fe XV at 284.3 Å. Above 340 Å the photographic spectrum is largely second, third and fourth order, and the only first-order line which was definitely present was Mg IX, at 369 Å.

The next important data were obtained when two Aerobee-Hi rockets were launched in May 1963. The first (May 2) was a scanning, grazing-incidence monochromator flown by Hinteregger and colleagues of AFCRL (ref. 50) using a reduced scanning rate and thus resulting in a greatly improved signal to noise ratio. Replacing the tungsten photocathode with LiF deposited on a glass substrate extended the long-wavelength-blind range and increased the quantum efficiency at shorter wavelengths. The spectra extended far beyond the previous limit of 170 Å, and lines were detected down to 65 Å. The spectrum still showed a sudden dropoff below 170 Å; therefore the tungsten cathode could be ruled out as a cause.

On May 10, 1963, the grazing-incidence spectrograph of Austin, Purcell, and Tousey (ref. 41) was reflown with decreased slit width and a higher speed diffraction grating. Approximately 125 lines were clearly present above 170 Å, and some 50 lines (though not all resolved) between 45 Å and 170 Å. In this region the data differ from the photoelectric record, probably due to the different spectral efficiency characteristics of the instruments.

The extreme ultraviolet emission lines which have been identified in the records from these flights have recently been tabulated by Zirin (ref. 51). The following criteria were used for identification:

(1) Coincidence within 0.1 Å

(2) A strong and probable transition in an abundant ion

(3) Observation of other strong lines from the ion, in approximately the right intensity ratios.

INTERPRETATION

Spectral Line Intensities

This section is concerned primarily with the emission-line solar spectrum as obtained by rocket flights during the past 6 years. Satellite data and additional interpretation will be considered later.

An excellent review of these data has been provided by Pottasch (ref. 52). Emission lines from 1900 Å to about 15 Å are considered. The lines whose intensities are known are due principally to ions with ionization potentials ranging from 13 eV to 600 eV. These lines come from a region in the solar atmosphere where the temperature changes from about 15 000° K to several million degrees. This is the "transition region," which has been only poorly understood from the past optical measurements. For convenience the observed lines which have been identified are reproduced in tables I and II (from Pottasch's review). A few belong to a stage of ionization not listed and whose energy levels are at present unknown.

Table I.—*Observed Emission-Line Intensities*

[From ref. 52]

Wavelength, Å	Intensity, ergs/cm²/sec			Probable identification
	Oct. 10, 1946	Aug. 23, 1961	July 10, 1964	
1892.03	0.08	.....	.....	Si III
1862.78	.04	.....	.....	Al III
1854.72	.02	.....	.....	
1817.42	.45	.....	.....	Si II
1808.01	.15	.....	.....	
1670.81	.08	.....	.....	Al II
1657.00	.16	.....	.....	C I
1640.47	.07	.....	.....	He II
1561.40	.09	.....	.....	C I
1550.77	.06	.....	.....	C IV
1548.19	.11	.....	.....	
1533.44	.041	.....	.....	Si II
1526.70	.038	.....	.....	

Table I.—*Observed Emission-Line Intensities*—Continued

Wavelength, Å	Intensity, ergs/cm²/sec			Probable identification
	Oct. 10, 1946	Aug. 23, 1961	July 10, 1964	
1402.73	0.013	.....	.....	Si IV
1393.73	.030	.....	.....	
1335.69	.050	.....	.....	C II
1334.52	.050	.....	.....	
1306.02	.025	.....	.....	
1304.86	.020	.....	.....	O I
1302.17	.013	.....	.....	
1265.04	.020	0.03(?)	.....	Si II
1260.66	.010	.03(?)	.....	
1259.53	.002	.....	.....	
1253.80	.0014	.....	.....	S II
1250.50	.0007	.....	.....	S II
1242.78	.003	.....	.....	N V
1238.80	.004	.....	.....	
1215.67	5.1	4.4	4.4	H Ly
1206.52	.030	.08(?)	.071	Si III
1201.0	.0015	.....	.....	
1194.2	.0015	.....	.....	S III
1190.2	.0015	.....	.....	
1175.70	.010	.03	.042	C III
1085.71	.006	.007	.009	N II
1073.00	.0008	.....	.....	S IV
1062.67	.0008	.....	.....	
1037.6	.025	.028	.025	O IV
1031.9	.020	.040	.036	
1025.72	.060	.050	.045	H (2) Ly
991.6	.010	.01	.....	N III
989.79	.006	.....	.007	
977.03	.050	.08	.081	C III
972.5	.....	.....	.011	H (3) Ly
949.74	.010	.008	.005	H (4) Ly
944.52	.0013	.0015	.....	S VI
937.80	.005	.005	.004	H (5) Ly
933.4	.0029	.0024	.....	S VI
834	.....	.016	.013	O II O III
790.10	.....	.013	.009	O IV
787.71	.....	.012	.008	O
786.48	.003	.....	.....	S V
780.3	.....	.0065	.004	Ne VIII
770.4	.....	.013	.011	
765.14	.....	.0077	.006	N IV
760	.....	.004	.....	O V
718.5	.....	.003	.....	O II
703	.....	.006	.007	O III

Table I.—*Observed Emission-Line Intensities*—Continued

Wavelength, Å	Intensity, ergs/cm²/sec			Probable identification
	Oct. 10, 1946	Aug. 23, 1961	July 10, 1964	
686.34	.....	0.003	.....	N III
629.73	.....	.045	0.056	O V
625.3	.....	.013	.....	Mg X
609.8	.....	.025	.....	
599.60	.....	.003	.....	O III
584.33	.....	.055	.053	He I
572.34	.....	.001	.....	Ne V
569	.....	.0025	.....	Ne V
562.81	.....	.0015	.....	Ne VI
558.60	.....	.0015	.....	
554	.....	.01	.....	O IV
550	.....	.0012	.....	Al XI
542.07	.....	.002	.....	Ne IV
537.02	.....	.0074	.....	He I
525.80	.....	.0017	.....	O III
521.1	.....	.010	.....	Si XII
515.61	.....	.002	.....	He I
508	.....	.003	.....	O III
499.3	.....	.021	.....	Si XII
465.2	.....	.013	.....	Ne VII
435	.....	.007	.....	Mg VII
430	.....	.0045	.....	Mg VIII
417	.....	.0075	.....	Fe XV
411.1	.....	.002	.....	Na VIII
401	.....	.008	.....	Mg VI
392.4	.....	.001	.....	Al IX
385.0	.....	.001	.....	
368.1	0.032	.....	.031	Mg IX
365.9	.012	.....	.....	Fe XIV
361.7	.018	.....	.....	Fe XVI
356.1	.009	.....	.....	Si X
352.9	.01	.....	.....	
348.9	.013	.....	.....	
347.4	.007	.....	.....	Si X
344	.007	.....	.....	Fe XIV
339.5	.005	.....	.....	
336.6	.028	.....	.....	Fe XVI
332.9	.002	.....	.....	Al X
328	.003	.....	.....	
319.8	.004	.....	.....	
315	.01	.....	.....	
308.6	.....	.00045	.....	
307.2	.....	.004	.....	
303.78	.24	.25	.25	He II
303.4	.....	.....	*.025	Si XI

*The Si XI line was separated from the neighboring He II line by the NRL in a flight on May 10, 1963.

Table I.—*Observed Emission-Line Intensities*—Continued

Wavelength, Å	Intensity, ergs/cm²/sec			Probable identification
	Oct. 10, 1946	Aug. 23, 1961	July 10, 1964	
296.2	.....	0.004	.....	SiIX
292.8	.....	.0025	.....	Si IX
284.3	0.44	.021	.....	Fe XV
281.1	.....	.0006	.....	
278.7	.....	.0006	.....	P XII
277.05	.....	.003	.....	Si VIII
272.0	.....	.003	.....	Si X
266.38	.....	.0007	.....	N V
264.4	.....	.004	.....	S X
259.3	.....	.003	.....	
256.32	.....	.015	.....	He II
253.8	.....	.002	.....	Si X
251.8	.....	.0037	.....	
249.1	.....	.0015	.....	Si VI
246.0	.....	.0020	.....	
244.91	.....	.002	.....	C IV
243.03	.....	.0037	.....	He II
241.7	.....	.0075	.....	
238.57	.....	.0017	.....	O IV
237.33	.....	.002	.....	He II
232.5	.....	.00083	.....	He II
225.0	.....	.....	0.007	
216.92	.....	.....	.007	Si VIII
211.7	.....	.....	.009	
203.9	.....	.....	.008	
202.5	.....	.....	.014	
198.6	.....	.....	.0014	S VIII
195.3	.....	.....	.04	
193.6	.....	.....	.025	
188.5	.....	.....	.05	
182.4	.....	.....	.017	
180.6	.....	.....	.09	
177.3	.....	.....	.08	
174.7	.....	.....	.09	
173.1	.....	.....	.0064	O VI
172.17	.....	.....	.003	O V
171.3	.....	.....	.09	
154.0	.....	.....	.0043	O V
150.12	.....	.....	.0045	O VI
148.3	.....	.....	.017	
115.8	.....	.....	.0033	O VI
103.6	.....	.....	.0094	Fe IX

Table II.—*List of Resonance Lines*

[From ref. 52]

Ion	Wavelength, Å	Isoelectronic sequence	f-value	Intensity, ergs/cm²/sec
C II	1335. 7; 1334. 5	Boron	0. 32; 0. 32	0. 10
C III	977. 0	Beryllium	0. 74	0. 08
C IV	1550. 7; 1548. 2	Lithium	0. 1; 0. 02	0. 06; 0. 11
N II	1085	Carbon	0. 70	0. 009
N III	991. 5; 989. 8	Boron	0. 27; 0. 27	0. 012
N IV	765. 1	Beryllium	0. 59	0. 0077
N V	1242. 8; 1238. 8	Lithium	0. 08; 0. 17	0. 002; 0. 004
O II	833	Nitrogen	0. 75	0. 016
O III	834	Carbon	0. 61	0. 016
O IV	790. 1; 787. 7	Boron	0. 22; 0. 22	0. 013; 0. 012
O V	629. 7	Beryllium	0. 48	0. 045
O VI	1037. 6; 1031. 9	Lithium	0. 07; 0. 135	0. 014; 0. 026
Ne IV	542	Nitrogen	0. 36	0. 002
Ne V	570	Carbon	0. 6	0. 0035
Ne VI	562. 8; 558. 5	Boron	0. 17; 0. 17	0. 003
Ne VII	465. 1	Beryllium	0. 47	0. 013
Ne VIII	780. 3; 770. 4	Lithium	0. 05; 0. 105	0. 006; 0. 013
Na VIII	411. 1	Beryllium	0. 45	0. 002
Mg VI	400	Nitrogen	0. 36	0. 008
Mg VII	432	Carbon	0. 45	0. 011
Mg VIII	430; 436	Boron	0. 28	0. 011
Mg IX	368. 1	Beryllium	0. 4	0. 032
Mg X	625. 3; 609. 8	Lithium	0. 045; 0. 085	0. 013; 0. 025
Al III	1862. 8; 1854. 7	Sodium	0. 61; 0. 32	0. 04; 0. 02
Al IX	392. 4; 385. 0	Boron	0. 25	0. 002
Al X	332. 9	Beryllium	0. 35	0. 002
Al XI	550. 0	Lithium	0. 08	0. 0012
Si II	1817. 2; 1808. 0	Aluminium	0. 6; 0. 6	0. 45; 0. 15
Si III	1206. 5	Magnesium	1. 62	0. 049
Si IV	1402. 7; 1393. 7	Sodium	0. 28; 0. 57	0. 013; 0. 03
Si VI	249. 0; 246. 0	Fluorine	0. 34	0. 003
Si VIII	319. 8	Nitrogen	0. 15	0. 004
Si X	356. 1; 347. 4	Boron	0. 09; 0. 09	0. 009; 0. 007
Si XI	303. 4	Beryllium	0. 39	0. 03
Si XII	521. 1; 499. 3	Lithium	0. 035; 0. 075	0. 01; 0. 021
P XII	278. 7	Beryllium	0. 38	0. 006
S II	1250–60	Phosphorus	1. 1	0. 004
S III	1190–1202	Silicon	1. 13	0. 0045
S IV	1073. 3; 1062. 7	Aluminium	0. 8	0. 0016
S V	786. 5	Magnesium	1. 4	0. 003
S VI	944. 5; 933. 4	Sodium	0. 29; 0. 58	0. 0014; 0. 0027
S VIII	198. 6	Fluorine	0. 13	0. 0014
S X	264. 3; 259. 4	Nitrogen	0. 12; 0. 08	0. 004; 0. 003
Fe IX	103. 6	Argon	.....	0. 0094
Fe XIV	366; 344	Aluminium	0. 1; 0. 15	0. 012; 0. 007
Fe XV	284. 3	Magnesium	1. 1	0. 032
Fe XVI	361. 7; 336. 6	Sodium	0. 16; 0. 29	0. 018; 0. 028

In general, the energy in these lines may be produced by collisional excitation or radiative recombination. In the transition region, however, collisional excitation is the important process since radiative recombination is much slower, by a factor of up to 10^4 for resonance lines. The rate of excitation by collision becomes LN_eN_Z, where $L(=\overline{v\sigma_{ex}})$ is the collision rate per electron and ion, v the electron velocity, N_e the electron density, and N_Z the density of the Z stage ion. Since the Sun's outer atmosphere is almost completely ionized, N_e is related to the hydrogen density N_H by the approximation

$$N_e = 1.2N_H$$

The degree of ionization can be expressed by (N_Z/N_E) and the abundance by (N_E/N_H), where N_E is the total density for the element E in all stages of ionization.

At electron densities below $10^{10}/cm^3$, the principal means of recombination from an ionized state is by radiative recapture rather than by three-body collision. Thus the ratio of the population of a single stage of ionization N_{i+} to that of the immediately lower stage N_i is given by

$$\frac{N_{i+1}}{N_i} = \frac{C_{i,i+1}}{\alpha}$$

where $C_{i,i+1}$ is the rate of collisional ionization and α is the recombination coefficient. A useful set of ionization equilibrium calculations has been made by House (ref. 53), who treated all elements from H to Fe and all ions from $Z=1$ to 20.

In analyzing the above observations, it is assumed that each collisional excitation from the ground state of an ion to the lowest excited state from which an electric dipole radiation is allowed results in the emission of a resonance-line quantum. The intensity E (erg/cm^2/sec) of a resonance line emitted from the Sun is

$$E = 1/2 \frac{h\nu}{4\pi R^2} \int NC\, dV$$

where $h\nu$ is the energy of a single quantum, C is the collisional excitation rate, N is the ground state density of the ion in question, R is the solar radius, and the integration is performed over the

entire volume V above the solar limb. After rearrangement, the quantity

$$\frac{N_E}{N_H} \int_R N_E^2 \, dh$$

emerges as an important indication of the atmospheric structure, where the "height" h is an element of volume divided by the area of the Sun. When this quantity is plotted as a function of temperature for various elements, the curves are essentially the same except that they are displaced from one another along the ordinate. Pottasch (ref. 52) plots this expression versus temperature for all the ions listed in table II, after the relative abundance of each element has been adjusted so that as little scatter as possible from a common curve is obtained. The scatter is generally within 40 percent, with no differences of isoelectronic sequences greater than this amount being observed.

The relative abundances obtained in this way, when compared with the photospheric abundances found by Goldberg et al. (ref. 54), show no difference greater than a factor of two for half the elements. For the four metals Mg, Al, Si, and Fe, this analysis gives a greater abundance than does the photospheric analysis.

Line Profiles

Another set of data treating the same region and obtained with rocket-borne equipment is that resulting from the study of emission line profiles. Profiles of the first two lines of the Lyman series of hydrogen were observed in 1959, 1960, and 1962; the 1959 data pertained to a quiet region of the active Sun and that of 1962 to a quiet-Sun condition. Self-reversal is deeper for the quiet Sun, and clearly the lines are formed in a region where the optical depth is large.

At present the only theoretical discussion of the hydrogen Lyman-alpha profile is that due to Morton and Widing (ref. 55), which is based on a study of the transfer of radiation in a simple two-level atom. Naturally many approximations had to be made, and it was necessary to assume that the line was formed in an atmosphere of constant density and with only a guess as to the temperature gradient. Further, no velocity fields were used. Under these conditions, a profile was made to fit the observed

shape in the core of the line successfully, but the fit was very poor in the wings. The fit is obtained by adjusting the temperature and density where the line is formed so that the separation of peaks and absolute intensity can be matched. For the normal regions of the Sun the electron density and temperature found are $N_e = 3 \times 10^9/cm^3$ and $T_e = 90\,000°$ K. This does not seem completely reasonable since to obtain an optical depth of 10^2 for the center of hydrogen Lyman-alpha at this density, a scale height of 500 000 kilometers is needed, an unreasonably large number. Obviously, the interpretation of the Lyman profiles requires further study, and radio-frequency observations may provide some of the information required for interpretation.

Structure of the Quiet Solar Atmosphere

The physical problems of the Sun's outer atmosphere have been separated into almost independent studies of the chromosphere and the corona. The pressure and temperature differences between these layers are so large that any attempt to interpolate between them usually fails. The situation is made worse by ambiguities concerning both the top of the chromosphere and the bottom of the corona. Zirin and Dietz (ref. 56) have suggested that the individual spicules provide most of the optical radiation from the top of the chromosphere and that the regular chromosphere is not observed higher than about 2000 kilometers from the base of the chromosphere. On the other hand, there are no observations giving the height of the lowest part of the corona. All that is known is that it is below 10 000 kilometers.

It can be said with some certainty that the transition layer must be quite thin. This conclusion is based on the absence of all the intermediate ions of Ne, Mg, and Si, with ionization potentials between 100 and 300 eV. Since only maximum values for the intensity of these "missing" lines can be given, we can infer that the transition region, having a temperature between 50 000° and 10^6 °K, has less than one-tenth as many atoms as the corona or the higher temperature portion of the chromosphere. However, the fact that spicules and prominences are features of this region makes further analysis difficult. At present many dif-

ferent models are being tried in an effort to explain the observations.

Centers of Activity and Flares

The variations in extreme ultraviolet radiation and its correlation with solar activity make it clear that a considerable portion of this emission comes from active areas of the Sun. It is also clear that these changes can be divided into two types: (1) slow variations with a life of several days, probably thus influenced by solar rotation, and (2) sudden variations associated with flares. It is the slowly varying emissions that come from solar active centers, which may be plages or coronal condensations. Although the geometry of active areas is likely to be complex, little else can be done but to regard them as horizontally stratified, with outwardly increasing T and decreasing N_e. Data required for calculations and analyses of these regions is rapidly improving and much more will be done in the near future.

Flares introduce additional problems. In the first place, they are more variable in shap, time, and character than other features. Secondly, the detailed line spectrum of flare emission below 10 Å has not yet been observed. In addition, the electrons in flares may not have a Maxwellian velocity-distribution. Until emission lines characteristic of flares (< 10 Å) are observed, the best hope of progress is to calculate emission from assumed models and compare it with available unresolved spectroscopic observations. Such a flare analysis has been made by Pounds et al. (ref. 57). By interpreting the spectral distribution as thermal emission, they obtain flare temperatures up to 10^7 °K. However, by assuming the radiations to be dominated by line emissions at the long wavelength end of the observed region, higher temperatures could be calculated. Certainly much further development is needed for treatment for all of these features.

Laboratory Astrophysics

One of the primary difficulties in the analysis of the solar extreme ultraviolet spectrum is the proper identification of spectral lines. Laboratory wavelengths, intensities, and identifications are not available for the vast majority of the lines observed. Theoretical identification often requires uncertain extrapolations

from the last well-calculated or observed energy level separation. Improvements in the techniques of spectroscopy, image formation, and photometry for this spectral range would be of great benefit.

Values of oscillator strengths and collision cross sections are also required for all atoms and ions whose spectral lines are present. It is not sufficient to know these parameters for just the immediate levels from which the spectral lines arise. Accurate rate processes must be known for all transitions important in establishing the equilibrium configurations of the atom. Laboratory measurements and theoretical calculations must be extended to supply these data.

chapter 5

Mapping the Sun's Soft X-Ray Spectrum

THE COMPLETE MAPPING of the solar X-ray spectrum is a complex problem, for it is necessary to obtain simultaneously wavelength and spatial and temporal resolution of radiation whose flux is low. During the past 6 years measuring techniques have gradually improved: the early detection and crude wavelength resolution measurements using the newer techniques have determined the shape of the short wavelength end of the spectrum and demonstrated the hardening of the spectrum in the presence of flares and solar disturbance. Pinhole camera measurements have shown that relatively small areas of the solar surface are responsible for most of the X-ray flux, and other measurements have shown the variable nature of the flux. Satellite measurements have enabled the flux variations to be observed over long periods and correlated with simultaneous measurements in the visible and ultraviolet regions, with radio bursts, and with ionospheric phenomena.

PREDICTION AND DISCOVERY

Historically, interest in extraterrestrial X-radiation arose from attempts to understand the mechanism of maintenance of the E-layer in the ionosphere, since energies of at least 12 eV are needed to ionize the atmospheric constituents, energies which cannot be explained on the basis of a Planckian radiator at the photospheric temperature.

Hulbert (ref. 58) and Vegard (ref. 59) suggested that solar X-rays might be responsible for the E-layer ionization. Edlen (ref. 60) identified certain coronal lines as being caused by elements in highly ionized states and Hoyle and Bates (ref. 61) estimated that a flux of between 10^{-2} and 10^{-1} erg/cm^2/sec would be required at wavelengths of about 40 Å to account for the E-layer.

The first positive identification of extraterrestrial soft X-rays was provided by Burnright (ref. 4) using photographic emulsion and filters flown on captured V–2 rockets. Further flights with different filters showed that X-rays were present in the 8–16-Å region and beyond 111 Å, limitations being set by absorption edges in the filters.

Friedman and his colleagues (ref. 62) at NRL flew photon counters and showed that an appreciable X-ray flux exists at wavelengths less than 10 Å but is negligible below 7 Å. Further rocket measurements in the 1952–58 period were made under various solar conditions by the NRL group (ref. 9) using photon counters and ionization chambers with filter windows. The fluxes found were as follows:

(1) <8 Å, 10^{-5} to 1.5×10^{-2} erg/cm^2/sec
(2) 8 Å–20 Å, about 10^{-3}erg/cm^2/sec
(3) 40 Å–100 Å, about 10^{-1} erg/cm^2/sec

Too few measurements were made to obtain reliable information about the variation with solar conditions, although more variation is apparent below 8 Å than for the longer wavelengths. For a review of this work, see also Friedman (ref. 63).

THEORIES OF THE X-RAY FLUX

Elwert Theory

The solar soft X-ray flux at middle wavelengths can be described by a blackbody distribution at temperatures around 10^6 °K, but it has absolute values many orders of magnitude less than for a Planck radiator. Elwert (ref. 64) made theoretical estimates of the solar soft X-radiation by considering the free-free and free-bound bremsstrahlung and excitation-recombination radiation from coronal electrons. This gives continuum and line spectra, and Elwert considered the radiation from the various constituents of the corona including highly ionized elements, at the short wavelength end. By comparing the relative intensities of visible and ultraviolet coronal spectral lines, estimates were obtained of the coronal temperature from the known line transi-

tion probabilities. Temperatures of the order of 10^6 °K were obtained. The ionization equilibrium, electron densities, and radiation spectrum were calculated. Order-of-magnitude agreement with experimental flux levels was obtained. Acton has criticized Elwert's calculations on the basis of revised abundances, inadequacy of the Born approximation for collisional excitation cross sections, and the contribution of recombination to the ionization equilibria.

Synchrotron Radiation

Stein and Ney (ref. 65) have calculated the continuum flux resulting from the synchrotron process in an attempt to estimate the radiation of flares at all wavelengths. They found that reasonable magnetic fields and electronic energy spectra similar to the observed proton spectra could account for the radiofrequency and visible continuum measurements. Under these conditions, however, synchrotron radiation is negligible at soft X-ray wavelengths. Very high fluxes of very energetic electrons would be required to produce any significant synchrotron X-ray emission.

Inverse Compton Effect

The scattering of low energy photons by relativistic electrons has been suggested by Schklovsky (ref. 66) to account for the hard component of solar flare X-rays. In an interaction known as the "inverse Compton effect," the electron loses energy to the photon, changing the latter's effective wavelength. Schklovsky calculated the electron energy distribution necessary to account for the observed X-ray fluxes and found it in agreement, within an order of magnitude, with that estimated from the optical spectra of flares. Acton has criticized this theory on the basis of balloon observations of the hard X-ray flare spectrum.

Fluorescence Radiation

The classic case of fluorescence radiation involves the ionization of an atom by removal of an inner shell electron by bombardment with energetic electrons. A fluorescence transition occurs when an outer shell electron drops into the inner shell. Acton (ref. 67) calculated fluorescence radiation for Fe, S, and Ne, and

found it negligible in comparison with thermal radiation; however, the fluorescence mechanism may become significant in some nonthermal processes as, for example, in a plasma excited by 15 keV electrons.

Bremsstrahlung

Bremsstrahlung is the radiation emitted when energetic electrons are decelerated by collision with dense matter. The apparent drift velocities of electrons exciting type III radio bursts correspond closely to the energies of hard X-rays observed rarely with certain flares. Of course the radio bursts originate in upward-directed streams, while bremsstrahlung must result from electron impact at chromospheric and photospheric levels.

Microscopic processes for solar X-ray emission have not been investigated in any detail. There is considerable uncertainty in the values of opacity and cross sections used in calculations of the above mechanisms and in the ionization equilibrium calculations upon which these are based. Nevertheless, the basic processes are sufficiently well understood to serve as guides in the initial interpretation of solar X-rays observations.

FORMATION OF THE IONOSPHERE

The soft X-ray spectrum of the quiet Sun covers the region from about 10 Å to 100 Å and is absorbed in the Earth's atmosphere in a fairly well-defined region between 100- and 150-kilometer altitude, forming the E-layer of ionization. The shorter wavelength radiation penetrates farthest, but the exponentially increasing atmospheric density produces a fairly well-defined lower altitude limit to the ionizaton profile. During disturbed conditions higher energy X-rays are produced which lower the level of the ionized region. That the soft X-ray flux is primarily responsible for the ionized E-layer has been demonstrated by observation of the change in critical frequency for radio wave reflection from the ionosphere during disturbed conditions. The observed change, by a factor of 1.5, is in good agreement with a value of 1.6 calculated for the known maximum and minimum values of the solar X-ray flux. Furthermore, analysis of the ion composition of the E-layer indicates that the equilibrium

ions are those produced by X-rays rather than by ultraviolet radiation.

ECLIPSES AND SUDDEN IONOSPHERIC DISTURBANCES

Observation of the critical radio frequency during an eclipse indicates an inhomogeneous X-ray source distribution assuming that the E-layer is due to X-rays. The ionospheric eclipse is irregular because of masking and unmasking of the discrete sources of ionizing radiation. Rocket measurements during the eclipse of October 12, 1958 (ref. 25), showed 10 to 13 percent of X-ray flux remaining at totality. The X-ray intensity of the corona was six times greater in the west limb, which contained several active plages, than in the east limb. Although it has been shown that the D-layer is produced mainly by the hydrogen Lyman-alpha radiation (ref. 68), this fact does not adequately explain the height decrease of the base of the D-layer during sudden ionospheric disturbances. Earlier rocket measurements showed enhancement of X-rays only during flares. Measurements by the NRL–SRI satellite have confirmed that the soft X-rays and not the hydrogen Lyman-alpha cause the flare SID events.

The most effective wavelengths in producing the D-layer are those less than 8 Å, and these may be increased by many orders of magnitude during flare events while total X-rays only double. Flare spectra have been measured (ref. 63), and the hardening of the radiation is probably due to suprathermal electrons (ref. 64) since the gas is cool. If the radiation were thermal, a temperature of 10^8 °K would be required to explain the observed radiation and the H-alpha line would not be emitted. The short wavelength limit during flare enhancement probably lies in the region of the Fe K series between 1 Å and 2 Å. It was also demonstrated that the ionized layer at 70- to 75-kilometer altitude, below the normal D-layer, would result from line emission at about 2 Å rather than from continuum.

ROCKET MEASUREMENTS

During the early observations by the NRL group before 1958, crude measurements were made of the X-ray spectrum in three

bands by using different counter gas fillings and windows (ref. 9). Variation of the X-ray flux with solar conditions was also noted. During the following 6 years, knowledge of the soft X-ray flux has been increased by a number of rocket flights, notably by the NRL group, the Leicester and London University groups, and a Russian group.

These measurements have mapped the X-ray spectrum in more detail, in particular at the short wavelength end, and flights under various solar conditions have enabled a start to be made on the difficult, but important, process of correlating X-ray flux with visible solar phenomena. Cutoff of the flux below about 10 Å is observed under quiet solar conditions, but the flux in this region increases by many orders of magnitude during flares, although the increase is much less at a wavelength of 50 Å. (See fig. 9.) During flares the short wavelength limit extends down to about 2 Å and a strong correlation exists between the solar activity and the flux at short wavelengths. At sunspot minimum the solar X-ray flux has a total value of about 0.1 erg/cm^2/sec and can be fitted to the Planck distribution for a temperature of 5×10^5 °K. The flux increases to about 1 erg/cm^2/sec at sunspot maximum under quiet conditions.

In April 1960 the NRL group obtained the first X-ray pinhole camera picture of the Sun (ref. 5) from an Aerobee rocket, giving a resolution of about 0.1 solar diameter with a pointing accuracy

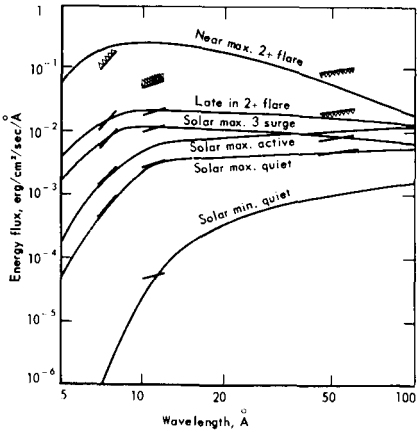

Figure 9.—Solar X-ray emission for various solar conditions.

of 1 arc-minute. Accidental rotation of the camera during the exposure through 160° about the pointing axis smeared the point images into arcs. In spite of this smearing, the X-ray sources can be seen to correspond with the bright plages on simultaneous calcium K-line photographs. It was concluded that the X-ray sources were smaller than the plage areas. The brightest X-ray source had 70 times the background intensity, and less than 5 percent of the area of the hemisphere was responsible for 75 percent of the X-ray emission. The mean solar diameter in X-rays is about 6 percent greater than the optical diameter, a difference of about 40 000 km.

A radioheliogram of the solar emission at 3300 Mc/sec, obtained at Stanford University, is similar to the X-ray heliogram when the former is rotated through 160° and photographed. However, the X-ray photograph shows greater contrast, which is interpreted as being due to enhanced X-ray line emission from active coronal regions. The photograph also showed that most of the X-ray emission originated in relatively small volumes of condensed coronal material coinciding with magnetically active plage regions at a higher temperature than the surrounding atmosphere. Line spectral measurements between 10 Å and 25 Å were made by the NRL group (ref. 69) using a Bragg crystal spectrometer carried in an Aerobee rocket. The spectrum was uncollimated so that line widths gave a direct measure of the angular width of the line-emitting region. Eighty-five percent of the integrated flux in this region was due to emission lines. Emission lines of highly ionized states were identified; namely, Fe XVII, O VII, O VIII and N VII. The narrowness of the Fe XVII and O VIII lines indicated that they originate in active regions of the same dimensions as plages; the remaining lines are broad as if from the whole solar disk.

The use of crystal spectrometers, together with the use of grazing-incidence telescopes for obtaining solar images, is a relatively new application in solar physics. Both techniques are important for they extend the wavelength and spatial resolution respectively by at least an order of magnitude over previous methods. Crystal spectrometers have been developed by the groups at Goddard Space Flight Center, at NRL, and at Leicester

209-916 O—66——5

and London Universities, and have been flown on rockets (1964) in their own right or as developmental projects for the OSO and AOSO programs. Grazing-incidence optics have also been rocket tested by the Goddard Space Flight Center (ASE) and the Leicester and London groups. Further rocket flights are scheduled for these instruments in 1965.

chapter 6

Evidence of Solar Hard X-Ray Emission

THE FIRST OBSERVATION of hard solar X-rays was made by balloon by Peterson and Winckler (ref. 70) in March 1958. Solar flare X-rays of energy greater than 20 keV penetrate the atmosphere to low altitudes. The flux was shown to be a burst of less than 18 seconds' duration and of energy in the region of 0.5 MeV. Subsequent measurements have been made by balloon by Anderson, Winckler, Vette, and Casal of short bursts in the 20- to 150-keV energy range. Ionization, Geiger counters and scintillation counters have been used as detectors. The NRL group (ref. 71) has shown that the spectral distribution during a flare of importance 2+ fits a source temperature of 10^8 °K and an electron density of the order of $10^9/cm^3$.

In the March 1958 flare, an intense burst of 800 Mc/sec radio emission occurred, simultaneous with the X-ray burst, but preceding the flash phase of the flare. In a later event (August 11, 1960), the spectral distribution was close to that of the NRL measurement, and coincided with type III radio-noise bursts. The flare of September 28, 1961, was observed by Anderson and Winckler (ref. 72) in the 20- to 150-keV range and showed a "precursor" followed by a rapid rise and decay of flux, the decay being broken into three stages of about 1-minute duration each. Radio bursts at 9500 Mc/sec coincided with the X-ray pulse peak and the precursor, while type III radio noise bursts coincided with the breaks in the decay. The visible flare started 14 minutes before the X-ray flash and reached a maximum 8 minutes after it. Microwave emission at 2000 Mc/sec followed the H-alpha event quite closely, but had no distinct similarities with the X-rays.

The extreme variability in the isolated balloon measurements of flare characteristics showed that considerably more sampling was necessary. Therefore, satellites have been used for sub-

sequent measurements of the short wavelength end of the X-ray spectrum.

There has been considerable speculation concerning the source of the hard radiation. One suggestion is that it may be produced by high energy protons exciting plasma oscillations, but these protons would have to be of 100-MeV energy. De Jager has proposed that the type III radio bursts are excited by streams of electrons accelerated in the flare region and moving into the corona with energies of 10 to 100 keV; he has proposed that the hard X-rays are produced simultaneously. Kawabata found that the microwave emission coincident with large flares can be considered to consist of an intense single burst and a long-term enhancement of flux called a "post burst increase." He has compared flare X-ray fluxes with thermal models and attributes the 2–8 Å emission to thermal emission at a temperature of 2×10^7 °K, although for shorter wavelengths higher temperatures must be postulated to obtain the observed spectral distributions. It is necessary to combine both the thermal and electron bremsstrahlung component theories to more fully explain the observed flare X-rays.

chapter 7

Corona

ENERGY IS GENERATED in the interior of the Sun, transported to the surface, and then escapes. Were it not for a flux of mechanical energy in the outer layers of the solar atmosphere, the density would decrease rapidly above the photosphere and the temperature would be no greater than the photospheric temperature, about 5000° K. However, the mechanical energy gives rise to shock waves and is eventually degraded to thermal energy, causing the outermost layers to become very hot. This is the origin of the corona, which may be observed out to several solar radii during eclipses. The radiation from the corona is only about one part in 10^6 of the total radiation from the Sun, meaning that the corona is difficult to observe; however, observations of the inner corona may be made with a coronagraph. The corona may also be observed at X-ray, ultraviolet, and radio wavelengths. The interpretation of these observations is reviewed by Seaton (ref. 73).

CORONAL TEMPERATURE

The temperature of the corona, as deduced from ionization equilibrium, is about 6×10^5 °K. At that temperature Fe X is near maximum abundance and the higher states of ionization are proportionately less abundant. Relative abundances have sometimes been better explained by assuming the corona to be thermally inhomogenous, the temperatures of quiet regions being as low as 6×10^5 °K and disturbed regions as high as 1.2×10^6 °K (ref. 63).

X-ray emission data have yielded temperatures as low as 5×10^5 at solar minimum. Measurements of the profile of the Fe X red and Fe XIV green lines, however, generally give temperatures greater than 2×10^6 °K if thermal broadening is as-

sumed. Some of the discrepancy may be attributed to the fact that lower temperature measurements refer to the quiet minimum corona and higher temperatures to more excited regions.

De Jager and Kuperus (ref. 74), in discussing the mechanical energy flux of the Sun, found that dissipation of shock wave energy in a completely quiet Sun could not produce a corona temperature higher than 6×10^5 °K. They concluded that the Sun is never completely quiet and that local heating from magnetic fields persists even at solar minimum, sufficient to increase the average temperature by at least 10^5 °K. To reach a coronal temperature of 2×10^6 °K, however, would require a mechanical flux at the coronal base equal to 2 percent of the solar constant. Thus, microturbulence or Alfvén waves may play a role in producing the observed line profiles.

CORONAL GREEN LINE AND X-RAYS

The red (6374 Å) and green (5303 Å) lines are emitted by the ions Fe X (E_i=233 eV) and Fe XIV (E_i=355 eV), respectively, and originate in the corona. The red line is fairly uniformly distributed over the corona, but the green line is concentrated in centers of activity associated with sunspots. Because the green-line intensity has often been correlated with ionospheric variability, it is of interest to compare its behavior with the observed changes in X-ray emission. A comparison made during 1959 rocket measurements showed that a 13-fold increase in green-line intensity corresponded to a 19-fold increase in 8–20-Å X-ray flux.

It has been pointed out that over the interval from minimum to maximum of the past cycle, the average green-line emission varied by a factor of 8 to 10, due perhaps to an increase in both temperature and density of the active regions. This green-line variation correlates well with the sevenfold variation in total X-ray flux. The red line changed very little but clearly showed a maximum intensity at sunspot minimum. Presumably the temperature of the corona decreased at solar minimum to a value closer to the maximum excitation temperature of the red line.

OSO B CORONAGRAPH

The brightness of the sky prevents the corona from being seen far from the limb with a coronagraph. If such an instrument were placed above the Earth's atmosphere, it would, in principle, make possible the observation of the white light corona at all times. At balloon altitudes of about 30 kilometers, the sky is reduced to a brightness nearly as low as that during a total solar eclipse. Above 100 kilometers, except for possible airglow emissions, the sky brightness is effectively zero, offering no impediment to rocket or satellite-borne instrumentation. Accordingly, a Lyot coronagraph with an external occulting disk was designed for the OSO B satellite and tested on two Aerobee-Hi rocket flights in June 1963. Two instruments (both designed at NRL under contract to NASA) were flown at this time, one using photoelectric recording and the other photographic. The field covered by these instruments was from $R=3.5$ to $10\,R_\odot$.

These were the first records of the solar corona brightness for these values of R made without the aid of a total solar eclipse. The results were far from perfect, but they are consistent and show that considerable improvement will result when the use of a larger vehicle will permit the external occulter to be placed farther away. All of the photographs show greater brightness in the direction of the Sun's equator and the approximate direction of the Earth's ecliptic than at right angles. Of course this light is in part the zodiacal or F-corona. It appears probable, however, that a portion is true K-corona since the brightness over the Sun's south pole was greater than over the north. Pictures taken at the High Altitude Observatory during the eclipse of June 20, 1963, also show greater brightness over the south than the north polar region. The zodiacal light, on the other hand, is expected to be symmetrical from north to south.

The corona photographs were of no value closer to the Sun's limb than $R=3.5\,R_\odot$. This distance is a little beyond the outermost part of the corona photographed during the July 20, 1963, eclipse and resulted from the closeness of the occulter.

The photoelectric coronagraph completed two scans during the time available, the first in tangential and the second in radial polarization. The results are neither as smooth as one might

expect, nor do they show any clear-cut features such as streamers. The irregularities were partly produced by the electrical noise and partly by the foreign matter known from the photographs to be flying through the field of view. However, the general shape and the radial distribution are in agreement with the photographic records.

However, the polarization data obtained photelectrically are not in agreement with other work. At the inner edge of the region covered, the tangential component was brighter than the electrons. From R=5 to 11 R_0, however, the polarization was in the opposite sense to that measured by others, although the magnitude was not measured. Possibly this observation is not correct, although such a condition has been suspected. At present no explanation exists for this result.

All the data seem to suggest that the Moon can never quite be matched as an occulter. Probably, however, with a multiple disk occulter at 10 feet or more from the objective, an orbiting coronagraph will be able to monitor the white-light corona with at least as great resolution and sensitivity as can be realized from the ground during a total eclipse.

chapter 8

Satellite Monitoring of Solar Radiation

SOFT X-RAYS

THE NRL PIONEER ROCKET OBSERVATIONS of solar X-ray and flare X-ray emission clearly pointed out the vital need for continuous observation of the Sun's emission at wavelengths between 1 Å and 100 Å. The frequency of flares which emit X-rays, their unpredictability, and the rapidity with which they develop make necessary continuous observations with time resolution at least as good as 1 minute and distributed over several weeks. The long time period is of course necessary because active regions themselves are a source of the softer X-rays and evolve over a few days to a few weeks.

A high pointing accuracy (initially to about 1 arc-minute) is also highly desirable so that high resolution measurements can be made of the solar surface. The NASA OSO spacecraft have this pointing capability, and in addition a pointing capability in the wheel of 1° at a 2-rpm scan rate. This spacecraft provides an important means of obtaining the desired X-ray data. However, the long development time for such an elaborate spacecraft encouraged NRL scientists to go a different route.

A rocket cannot be launched quickly enough in response to the start of an optical flare to measure the interesting part of the X-ray flare. Moreover, the flight time of a rocket is not adequate to make measurements of the entire X-ray flare history, nor indeed even of the ultraviolet flare.

The earliest attempts to measure solar X-radiation from Vanguard III and Explorer VII did not succeed because of the overwhelming background radiation in the Van Allen belts, which saturated the X-ray detectors.

Solar Radiation I

The first successful solar monitoring satellite, called Solar Radiation I (SR I), was put into orbit in June 1960. To protect the X-ray photometers from charged particles, the NRL group used permanent magnets to deflect the particles from the detector window. SR I carried an ultraviolet photometer, an X-ray photometer and a photocell solar aspect sensor. The X-ray detector was an argon-filled ionization chamber with a beryllium window which gave a passband between 2 Å and 8 Å. The satellite spin exposed the detector for short intervals while the sensor monitored the satellite's attitude relative to the Sun. Data were recovered only by real-time telemetry to the NASA Minitrack network and to a few isolated stations. Consequently SR I provided solar observations only 1.2 percent of the possible time. These were transmitted during more than 500 data-acquisition passes between June and November 1960. Approximately 20 percent of these records indicated detectable X-ray flux in the 2 Å to 8 Å band. Apparently the shielding magnet was successful in protecting the X-ray photometer from Van Allen belt radiation, since no Van Allen belt modulation was detected in any of the SR I data. However, the magnet strongly influenced the satellite spin dynamics. The component of the permanent magnetic field along the spin axis coupled with the geomagnetic field to produce a torque which resulted in an 8-day precession. The changing spin rate coupled with this precession resulted in complicated satellite kinematics. Precession also affected the attitude so that the Sun was under observation by the satellite only 50 percent of the time that the satellite was in sunlight.

SR I provided the following significant X-ray measurements:

(1) The quiet Sun normally does not emit more than 6×10^{-4} ergs/cm^2/sec below 8 Å

(2) Some solar activity was usually visible when a large X-ray flux was observed below 8 Å in excess of the quiet-Sun threshold

(3) Some ionospheric effect (SID) could be detected when the X-ray flux in this band exceeded 2×10^{-3} ergs/cm^2 sec

(4) Significant changes in the X-ray flux can occur in times as short as 1 minute

(5) Other types of solar activity besides flares produce SID; included are active prominence regions, bright surges at the limb, and subflares at the limb.

Solar Radiation III

In 1961 the composite satellites SR III and Injun I were launched. SR III had two ionization X-ray detectors for the 2–8-Å and 8–14-Å bands, while Injun I (intended for energetic particle studies) had a mica-window Geiger counter originally intended to measure low-energy geoelectrons in the radiation belts. The counter also responded to the 2–14 Å X-ray band with a sensitivity which could be determined approximately.

The satellites did not separate but spun slowly together in orbit. However, it was possible to obtain data (Acton, ref. 67) from the detectors and some attitude information.

The combined results of the SR III and Injun I satellites can be considered in two separate categories: X-ray emission of the quiet Sun and X-ray emission of solar flares. For the sake of this discussion, Acton defined the quiet Sun as the condition prevailing between impulsive outbursts of optical or radio flare activity; in other words the X-ray intensity will, by definition, show no large changes in level from one observation to the next, or from one day to the next. The NRL pinhole photographs show that individual active regions play an important role in enhancing the total X-ray flux from the Sun. Thus, continuity of observations is essential to validate any measurement on the quiet Sun so defined. For this reason, nearly 60 percent of the observations by this combined satellite were made during only a 5-day period. Transient events are well distinguished from the slowly varying background flux; uncertainties relate to the differentiation between active region radiation and quiet-region radiation. One important result of Acton's analysis is that the microwave (2800 Mc/sec) radiation and the X-ray radiation correlate in general, but not in detail. This is interpreted as the difference between the scales of source regions for X-rays and microwaves. The latter are conjectured to be optically thin on a microscopic

scale over an entire active center, though possibly optically thick in smaller structures (less than 2 arc-minutes). The microwave radiation source, on the other hand, is thought to be comparable in size to an entire active center because of the general distribution of electron densities of critical magnitude. The microwave emission is also less dependent upon small variations in the local temperature and density than is the X-ray flux.

The total quiet-Sun X-ray flux on a quiet day is of the order of 5×10^{-3} erg/cm^2/sec, ($\lambda < 14$ Å) and the coronal temperature must be about 2.3×10^6 °K. (The NRL pinhole photographs of the Sun indicate that most of this X-ray emission comes from the immediate neighborhood of active regions: coronal temperatures can be inferred from coronal emission-line profiles.) It is assumed that all the X-ray flux is produced from optically thick plasma at this temperature, isolated in the active centers and defined by the extended calcium K-line plages. In other words, Acton concluded that essentially all quiet Sun X-radiation comes from coronal enhancements and streamers which overlie the active regions roughly as delineated by the calcium K-line plages. Using the estimated electron densities and the observed extent of the emission regions, the intensity of 2800 Mc/sec radiation can be estimated from such a coronal condensation. The calculated flux is approximately 27 flux units, which is within a factor of 4 of the observed magnitude.

The observed short-term variations of the X-ray flux do not correlate neatly with variations in the microwave emission. One mechanism suggested by Acton to account for this discrepancy invokes high density regions of roughly 10^{25} cm^3, at 2.3×10^6 °K, with electron densities of the order of 10^{12}/cm^3. Regions as small as this could change their X-ray flux within the time scale observed, but variations in their radiofrequency emission will not be observable with existing equipment. Obviously the attendant visible light phenomena will lie at the threshhold of resolution, and conceivably they have not been observed. Only the "moustaches" appear dimensionally similar to such events. The X-ray emission from coronal prominences has not been observed by any of the spacecraft previously discussed. It is obvious from the very high temperatures prevalent in these plasmas

(as indicated by the Ca XV emission) that they must have intense X-ray emission.

SR III data relate to a number of flare-like events. For this discussion it is convenient to distinguish between thermally emitting flares, in which the X-ray emission results from local enhancement of electron density and temperature, and "nonthermal flares," in which the electron velocities depart significantly from a Maxwellian distribution and may be anisotropic. SR III observations confirmed the previously well-established fact that "thermally emitting" X-ray flares are more common. Such flares produce minor ionospheric effects or none at all. Another subclass of flares, those with an explosive phase, frequently produced nonthermal X-ray bursts. Studies on ionospheric effects may validate or qualify these crude satellite data on the relatively harder X-ray spectrum of the nonthermal flares. As a basis for discussion, Acton constructed two thermal models and one nonthermal model solar flare to provide comparison with the observational results. Acton concludes that both thermal and nonthermal processes are important and necessary to account for the optical, radio, and X-ray emission of flares.

Based on the radiofrequency and X-ray emission and depending also upon the relative roles of thermal and nonthermal processes and the energies of electrons involved, the following four categories of flux distribution can be defined:

(1) The coolest class of flares produce little if any X-ray or radio emission.

(2) Flares which produce small increases in X-ray intensity without marked hardening generally emit no strong microwave bursts and produce no notable ionospheric effects.

(3) Nonthermal radiation increases at wavelengths shorter than 2 Å, and thus the ionosphere disturbances become most significant. When the nonthermal component is noticeable but not at maximum intensity, microwave bursts will not be strong and will usually rise and fall gradually in intensity.

(4) The most extreme nonthermal events produce hard X-rays (greater than 20 keV) and X-ray enhancements up to two orders of magnitude above the quiet-Sun level. Such strong

bursts always produce ionospheric disturbances of the greatest magnitude and are accompanied by microwave bursts of the impulsive type.

Recently the SR VI, a further NRL solar radiation satellite, has been put into orbit and is working satisfactorily.

OSO I

NASA's Orbiting Solar Observatory program was designed to conduct experiments in solar physics, astronomy, and geophysics above the Earth's atmosphere from a platform pointing at the Sun. The OSO program consists of eight planned launches. OSO I was successfully launched on May 7, 1962, and will be followed by OSO II in 1965. A description of the scientific results of OSO I is given by Lindsay (ref. 75).

The OSO orbit is circular at an altitude of 300 nautical miles. The spacecraft (fig. 10) weighs 500 pounds and consists of a lower wheel section of nine wedge-shaped compartments, four containing control and recording equipment and five containing 30 pounds each of experimental equipment. This section rotates at 30 rpm to provide gyro stability and is mounted below a semicircular sail section which is kept pointing at the Sun to within 2

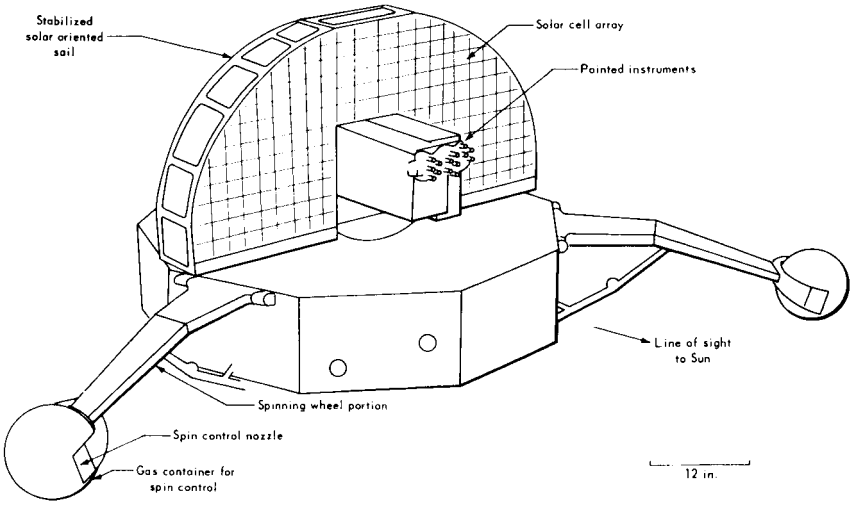

Figure 10.—Orbiting Solar Observatory.

arc-minutes. The sail can support two sets of experimental equipment weighing 50 pounds each. A more detailed description is given by Dolder et al. (ref. 3).

For X-ray measurements, the pointing section of OSO I contains a xenon-filled ionization chamber detector with a beryllium window 0.005 inch thick, developed by GSFC and sensitive to the range 1 Å to 8 Å (fig. 11). Scintillometers developed by GSFC, covering 0.51 MeV and 20–100 keV are also in the pointing section. In the wheel section are several gamma-ray detectors covering the 50-keV–3-MeV and 100–500-MeV regions. Results on slow variations and transient events in the 1-Å–8-Å region have been reported by White (refs. 76 and 77), and the observations of X-ray bursts in the 20–100-keV region by Frost (ref. 78). A slowly varying component of 1-Å–8-Å flux was

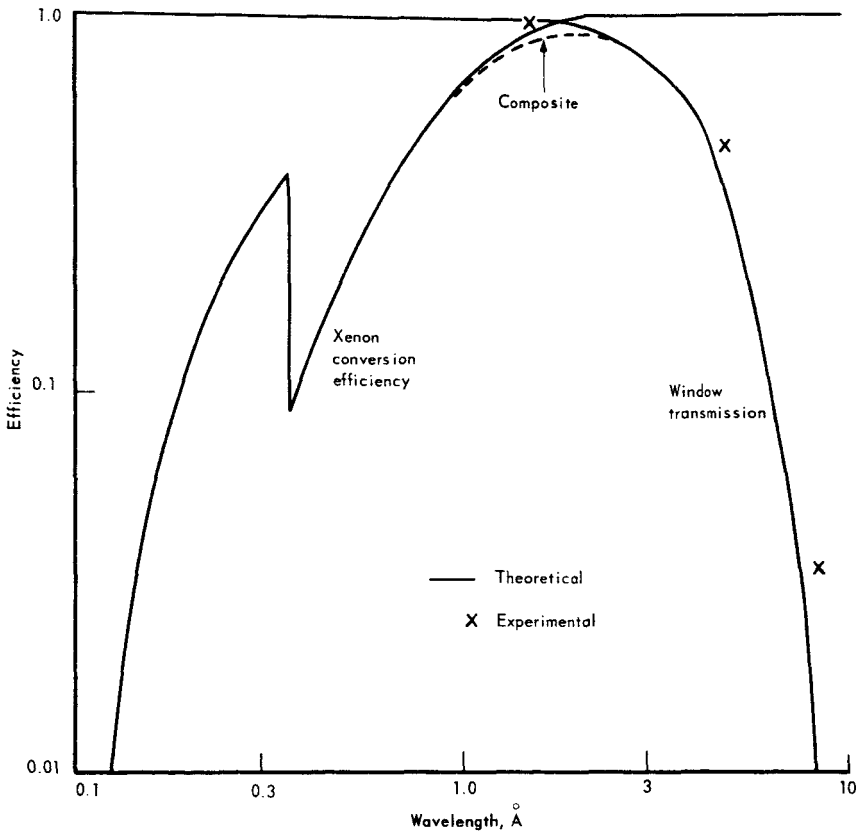

Figure 11.—OSO I ion chamber efficiency as a function of wavelength.

observed which correlates well with the slowly varying component of 2800 Mc/sec solar radiation (fig. 12). This radiation can be accounted for by localized sources having the same horizontal extent as calcium K-line plages with thicknesses proportional to their diameter and having an electron temperature of about 2.8×10^6 °K and an electron density of about 5×10^9 electrons/cm^3. A further conclusion is that the ratio of line emission to continuum emission is at least 10:1, and more probably 30:1, for these conditions.

In addition to a slowly varying component, transient events (X-ray flares) lasting from 10 minutes to a few hours were frequently observed (fig. 13). Correlations with H-alpha flares, with sudden ionospheric disturbances, and with 2800 Mc/sec transients have been investigated; the results show that as an indicator of local solar activity, the OSO I X-ray experiment was more sensitive by a large factor than indicators based on ionospheric effects or than indicators based on observations of solar flux in visible or radio wavelengths. X-ray flares were frequently observed associated in groups possessing a characteristic pattern.

Observations of the transient bursts of soft X-rays indicated that they could not be directly associated with microwave ob-

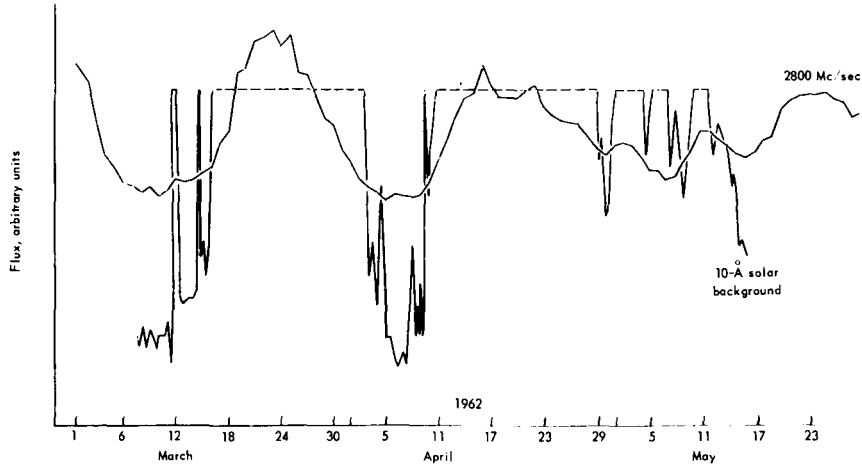

Figure 12.—Slowly varying components of 2800-MC/sec solar flux and of 1-Å–8-Å X-rays.

servations because of the extreme disparity in sensitivity of the two methods. However, the observations by Frost show a direct correlation between the 20–100-keV X-ray bursts and the microwave impulses together with sudden ionospheric disturbances. Frost concludes that the high-energy X-ray bursts are produced in the chromosphere by a nonthermal source.

Ariel I

The first joint U.S.–U.K. satellite Ariel I (or UK–I) was launched in April 1962. It carried a proportional counter detector with pulse height analysis giving a spectral resolution of approximately 2 Å in the 4–14-Å range (ref. 14). In the first 3 weeks of the life of this satellite, more than 150 measurements were made of X-ray flux over the entire wavelength range, representing averages over periods of 4 to 8 minutes, to a precision of about 10 percent (ref. 15). Even when flares were definitely known not to be occurring, on a few occasions the quiet-Sun X-ray flux varied by as much as 75 percent during an hour or less. There was some correlation between these small variations in the total flux and terrestrial observations of various solar in-

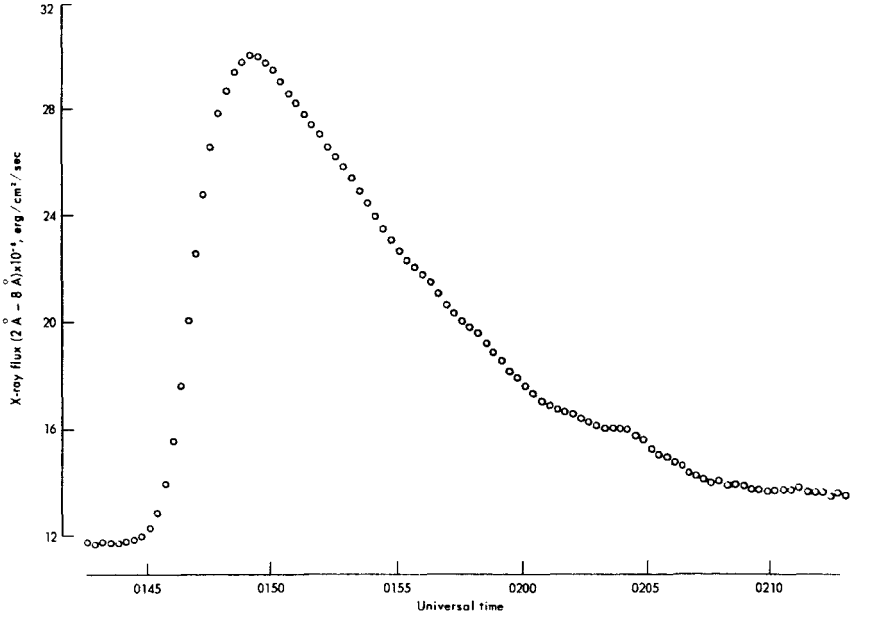

Figure 13.—Development of soft X-ray burst recorded by OSO I, March 8, 1962.

209-916 O—66——6

dices. Under quiet-Sun conditions, the intensity in this band decreased sharply at shorter wavelengths so that usually the two highest energy channels gave no reading at all. These spectra correspond roughly to 1.5×10^{6} °K. The integrated energies were estimated to be 3×10^{-3} ergs/cm²/sec for 8 Å to 14 Å, and 1.3×10^{-4} ergs/cm²/sec for wavelengths less than 8 Å. The values are more than 100 times greater than Elwert's estimated thermal radiation for a million-degree corona. Since Elwert's model was for an isothermal corona, the temptation is to postulate hotter localized regions at about 2 million degrees. The spectra, however, do not confirm this suggestion. Bowen has made an alternative suggestion that the spectrum of the quiet Sun in the 8-Å to 14-Å range is hybrid, consisting of a thermal component upon which are superimposed the nonthermal or quasi-thermal spectra of localized condensations.

Approximately 20 solar flares were observed in the X-ray region during the first 3 weeks. Generally X-ray flare spectra were confirmed not only as an intensification, but also as a hardening of the quiet-Sun spectrum. The magnitude of the flare X-ray emission varied considerably and did not correlate well with the importance of H-alpha flares. The high time resolution of the Ariel I spectrometer (0.1 to 1 minute) revealed that flare X-rays are emitted in brief flashes and do not occur as gradual brightenings to a single maximum and subsequent fading as is observed in the visible hydrogen spectrum. Flares exhibit considerable variety in their spectra. Thus, one example revealed gradients corresponding to a gray body at effective temperatures ranging between 2 and 3.8×10^{6} °K. Another well-observed example showed the relationship between spectral change in the flare X-rays and ionospheric responses. During the rise to maximum, the X-ray spectral distribution was essentially preflare in character so that the change was of intensity rather than of distribution. However, at the peak of the flash phase of this flare during the maximum of flare X-ray emission, the spectral distribution had hardened considerably. The spectral distribution corresponded to a plasma in quasi-equilibrium whose temperature rose from 10 to about 12×10^{6} °K during a 3-minute period. The X-ray flux at this phase was 2×10^{-3} ergs/cm²/sec. Electron

densities necessary to account for this flux can be calculated and correspond to those prevailing in the low corona or the chromosphere.

Other Satellite Measurements

Soft X-ray measurements have been made from a Russian satellite (ref. 17) using open-type photomultipliers as detectors and inserting various filters in sequence to select wavelength ranges. In this way various portions of the spectrum were selected from 1 Å into the ultraviolet. Measurements under quiet conditions were consistent with a blackbody spectral distribution at 0.9×10^6 °K, with little radiation below 1 Å, while under disturbed conditions the curve could be represented by an additional distribution at a temperature of 10^6 °K.

The Orbiting Geophysical Observatory, OGO I, launched in September 1964 contains scintillation counters to measure high energy solar X-rays.

Two X-ray monitoring satellities were launched in October 1963 as part of the Vela program. These are in high orbits, permitting almost continuous monitoring from 0.5 Å to 10 Å. Ten detectors are distributed over the surface of the spacecraft. Pairs of filters give separate spectral sensitivity bands of 1–20 keV (0.5–10 Å) and 3–20 keV (0.5–4 Å). During intense flares the flux measured by the thick filter detector was considerably less than that passing the thin filter. Many X-ray events were recorded, correlating in general with reported solar flares. However, on some occasions the observed flares exhibited no X-ray emission, and at other times there were X-ray events with no concurrent reported flares.

C. S. Warwick, in a private communication, has compared these Vela data with ground observations of X-ray effects upon the lower ionosphere. Flare X-rays create a sudden increase in electron density at heights corresponding to the D-layer and below. This response increases ionospheric absorption of cosmic noise (usually measured around 18 Mc/sec and called SCNA). Simultaneously, reflection of a VLF signal (say 16 kc/sec) becomes more efficient, and a sudden enhancement of atmospherics (SEA) is observed.

Warwick's comparison showed that all ionospheric events (SEA or SCNA) were accompanied by a measurable increase in solar X-rays. However, only about one-third to one-fourth of the Vela events were associated with reported ionospheric response. Both the 0.5–10-Å and the 0.5–4-Å detectors correlated with ionospheric responses when the flux exceeded well-defined thresholds. Since NRL's 1960 data showed a similar association for 2–8-Å X-ray flux while the 1961 data did not, Warwick concluded that radiation shorter than 10 Å is more important for producing ionospheric effects than that in the 10–20-Å range.

Warwick's analysis answers the question: to what extent can ground observations of X-ray events by their indirect effects supplant satellite-borne direct observations? SCNA data alone provide as many false alarms as real indications, unless corroborative data such as 3000-Mc/sec radio flux measurements are considered. About 80 percent of the bursts at these frequencies are accompanied by major X-ray events, and SCNA qualification would reduce the false alarm rate. For lesser X-ray events, no ground observations of indirect effects are sufficient to replace satellite measurements.

ULTRAVIOLET RADIATION

The NRL SR I Satellite

The first solar radiation monitoring experiments to be carried out from an orbiting vehicle were those of the NRL SR I Satellite (known also as Solar Radiation I, Greb I, and $1960\eta 2$). This was placed in orbit on June 22, 1960, and produced useful data for about 5 months.

The ultraviolet detectors were nitrous oxide ionization chambers with LiF windows, which responded to radiation from 1000 Å to 1350 Å. Difficulties encountered with these hydrogen Lyman-alpha detectors necessitated reliance on measurements made from rockets during this period for absolute calibration, and no hydrogen Lyman-alpha data were recorded after October 22, 1960. Records show that during the period from July 13 to August 3, hydrogen Lyman-alpha changes did not exceed 18 percent. The important result was the establishment of an

upper limit on possible variation of hydrogen resonance line intensity. During a disk flare of importance 2, the measurements clearly showed an upper limit in the flare emission of 11 percent of the total disk quiet-time flux. Intensity of flare hydrogen Lyman-alpha thus appears to be too low to play a significant role in the D-layer phenomena.

OSO I

More extensive solar monitoring experiments were made possible by the launching of OSO I in March 1962. The spectrometer used was a grazing-incidence grating instrument similar to Hinteregger's described earlier, having for the detector a Bendix magnetically focused strip-type photomultiplier. This instrument made continuous solar observations, whenever the satellite was in sunlight, for nearly three solar rotations in March, April, and May, 1962. During this period extreme ultraviolet spectra were obtained at the rate of one every 8 minutes, or approximately 7 per orbit, resulting in an estimated 7000 spectra being recorded for the first 2½ months of operation. These observations were followed by nearly 1 year of intermittent observations.

The spectrometer was designed to cover the wavelength range from 10 Å to 400 Å. However, below 100 Å the decreasing sensitivity, combined with an increase in scattered light made distinguishing a reliable spectrum impossible. The most reliable observations were thus obtained in the 150–400-Å region (ref. 79), and agree well with rocket observations in this region. The valuable additional information obtained demonstrates the use of satellite observations in identifying spectral lines and in studying changes in the solar corona with time, especially those changes associated with active centers and flares.

Line Identification

One of the difficulties of line identification in the far ultraviolet has been the richness of the emission-line spectrum. Making observations over a period of time and searching for groups of lines whose intensities have the same time dependence might solve this problem. This suggestion was based on the expectation that lines of one multiplet arising from closely spaced upper

levels will vary by the same amount with changes in solar activity, thus imposing an additional constraint which line identifications must satisfy.

This method was used in searching for the permitted transitions of Fe XIV. Lines of this ion are expected to be grouped into four multiplets between 200 Å and 400 Å. Examination of the time variations of lines in this region shows three groups with separations compatible with predicted splittings. Two of these groups may well correspond to the $2p–2p_0$ and $2s–2p_0$ transitions since they lie within 2 Å of the computed wavelengths. Two other lines, at 204 Å and 211 Å, have the same variation and probably correspond to the $2d–2p_0$ transitions. No other lines exhibit the same time dependence.

Having examined one set of lines, it is of interest to examine other lines of the same element, which perhaps belong to different stages of ionization. For example, those lines common to both the zeta discharge and the Sun may be iron lines. Essentially four groups of lines have been observed by the OSO I spectrometer according to the amplitude of the fluctuations. The group with somewhat less variation than the above Fe XIV lines may well originate in Fe XIII, as suggested by the similarity with those of another possible Fe XIII line at 364 Å. The remaining lines have been placed in two not completely distinct categories. The least variation is shown by a group of lines near 170 Å, and also by a possible Fe X line at 345 Å, indicating that these last two groups may originate in Fe X, Fe XI, and Fe XII, the smallest variation being associated with FeX.

To summarize the observations, those ions existing at lower electron temperatures generally vary less than those at higher temperatures. Since the variation depends upon solar activity, this will be mentioned before further discussions of these observations.

Variations of the Extreme Ultraviolet Spectrum With Solar Activity

The use of OSO I has permitted the acquisition of a solar extreme ultraviolet spectrum which can tentatively be associated with a corona disturbed by varying centers of activity. The closest approach to observation of a quiet Sun was obtained on March 11,

1962, when the observed face of the Sun had been free of disturbances for the preceding 6 months. An analysis of emission lines, made for the period from March 7 to April 5, shows that the lowest counting rates of the period were observed when the sunspot number was near zero and the calcium K-line plage area was also at a minimum.

It was also clear, however, that no exact correlation could be assumed to exist between the extreme ultraviolet flux and ground-based observations. Fe XV and XVI lines, for example, were lower on May 1 when the sunspot number was 49 than on May 15 when it was 15. Similarly, although the agreement between the radio data obtained at 2800 Mc/sec by the NRC and extreme ultraviolet coronal fluxes is sometimes remarkable, it is not truly consistent. A small maximum at 2800 Mc/sec on May 1 to May 5 does not appear at 284 Å, whereas on succeeding days a larger peak is observed at 284 Å than at radiofrequencies. The region under observation in May when a small maximum was observed at 2800 Mc/sec was a flare-producing center of activity roughly 1 solar rotation old, whereas the plages existing on the Sun on May 9 to May 15 are for the most part remnants of active centers four to five rotations old which were no longer sites of flare activity.

These observations suggest the necessity of having knowledge of the recent history of solar activity as well as current data to correlate extreme ultraviolet radiation with other information. The extreme ultraviolet emission lines each display individual features which vary from one line to another. In particular He line fluctuations, but not others, can sometimes be associated with the brightening of existing plages and the occurrence of radio noise storms at 169 Mc/sec as recorded in France.

The coronal lines of Fe XIV, Fe XV, and Fe XVI are strongly associated with plages, but they appear to have residual intensities even if the Sun shows no sign of activity. Although large fluctuations occur in the relationship of Fe XV to the plage area, the Fe XV emission is more strongly associated with plages than Fe XIV. Assuming that the regions of increased Fe XV emission are equivalent in area to the plages, a plage to quiet-Sun Fe

XV ratio of between 200 and 300 to 1 may be calculated. This quiet-Sun component may be associated with fine structure or it may be uniformly distributed; better spatial resolution is required to determine this. If both radiations are assumed to originate in the same region of the corona, a temperature of the order of 1.75×10^6 °K is obtained from the theory of ionization equilibrium. This temperature is to be compared with a value of 8×10^5 °K usually obtained for undisturbed portions of the corona.

To summarize the data on other extreme ultraviolet lines, those ions existing at electron temperatures below about 10^6 °K (lower stages of Fe, Si VIII through Si X, and Mg VIII and IX) show little association with active regions, while those ions existing above 10^6 °K show strong association with plages and active regions. It is not clear whether certain large increases in Fe XV and Fe XVI result from a combined increase of electron temperature and density over plages or whether localized regions in which these emissions might occur merely increase in number over plages. Better spatial resolution is required to determine how the smaller increases in intensity are distributed over the solar disk.

Flare Activity

The OSO I spectrometer observed transient events superimposed on the slow variations in the spectrum. Generally it is difficult to obtain reliable data for such events because the increase in radiation is small compared with the radiation from the entire disk and because the long time required to scan the spectrum (8 minutes) severely limits the time resolution for a particular spectral line. However, several tentative conclusions can be drawn from the data. In the first place, of all the extreme ultraviolet lines examined, the largest increase during the flares is associated with the ion having the highest ionization potential, Fe XVI. Secondly, even for this spectral line the increase is considerably less than for harder X-rays. For a flare of importance 2+, on March 13, 1962, the Fe XVI line at 335 Å increased by 60 percent, while the 1–10 Å ionization chamber output (ref. 80) increased by a factor of more than 3.

In general, the Fe XVI flux increases more than does that from Fe XV, thus altering the 355 Å/284 Å ratio. In many cases no change whatever is observed for the Fe XV flux during the flare. The 304-Å line shows an increase of about 10 percent approximately coincident with the optical flare. A 30 percent increase is observed in the 335-Å line, but only after a class II radio burst has occurred. No change is observed in the 284-Å line.

OSO I also monitored the total flux of hydrogen Lyman-alpha, providing data for a period during which five flares of optical importance 2 occurred. All hydrogen Lyman-alpha enhancements occurred mostly within the duration of the H-alpha flare. Apparently, there is no typical time dependence of the variation in hydrogen Lyman-alpha. The time of peak hydrogen Lyman-alpha enhancement does not necessarily coincide with the H-alpha flare maximum, but usually precedes it slightly.

The flare of March 22, 1962, provided the best observed hydrogen Lyman-alpha enhancement (ref. 81). It is unique among all the events in that the time course of the hydrogen Lyman-alpha enhancement was similar to that of a classic H-alpha flare. The time of hydrogen Lyman-alpha maximum coincided exactly with the reported optical flare maximum.

chapter 9

The Future Flight Program

SOLAR EXPLORER SATELLITE

THE IQSY SOLAR EXPLORER SATELLITE to be launched by NASA late in 1965 will perform continuous monitoring of solar X-rays. The orbit altitude will vary in the 650- to 1020-kilometer range, and the satellite will carry nine X-ray photometers. In concept the satellite is similar to the NRL Solar Radiation series, but it has facilities for data storage as well as direct transmission. Also, there is provision for reorientation of the spin axis so that the instrument viewing time is kept to a maximum. Data transmitted continuously is intended to be received by any convenient station.

ORBITING SOLAR OBSERVATORY

A total of eight launches has been approved for the OSO program; the remaining schedule showing two in 1965, one in 1966, two in 1967 and one each in 1968 and 1969. Payloads for OSO B through OSO E have been selected as of January 1965. OSO B and later spacecraft also include a Sun-scan raster 40 arc-minutes side and 1 arc-minute resolution. In the soft X-ray range the selected experiments include, specifically, a crystal spectrometer developed by NRL for the observation of solar flares and grazing-incidence spectroheliographs developed at GSFC/ASE and at Leicester and London Universities. In addition the flights will carry scintillometers developed at GSFC, Geiger counters developed at NRL and Leicester and London Universities, proportional counters developed at Leicester and London Universities, and ionization chambers developed at the University of Michigan and NRL.

The crystal spectrometer and spectroheliographs will be used to obtain detailed wavelength and spatial resolution of solar X-radiation and thus increase the knowledge of the nature of the

individual sources. The various ionization and scintillation detectors will provide continuous monitors of the radiation in specific wavelength bands so that studies and comparisons can be made over as large a variety of solar conditions as possible. Some additional soft X-ray measurements are also being made as part of the OSO program.

ADVANCED ORBITING SOLAR OBSERVATORY

The AOSO (fig. 14) is intended to make continuous, detailed, high-resolution studies of solar phenomena with considerably higher pointing accuracy than the OSO spacecraft. This spacecraft should enable much higher spatial resolution to be obtained in measurements of solar phenomena such as flares. It has a normal pointing accuracy of $\pm$ 5 arc-seconds of the radiometric center of the Sun, an offset point of similar accuracy within a 40 arc-minute square centered on the Sun, and two raster scans, one coarse and one fine. A total weight of 250 pounds is available for experiments.

Four launches have been planned so far, one in 1969 and three more during the next 3 years. Single launches following at yearly intervals have also been proposed. The program also involves the development of instrumentation for solar viewing in various wavelength ranges, including a high-resolution (5 arc-seconds) X-ray telescope by Lindsay and Giacconi (GSFC/ASE). At present, four experiments have been selected for the project, and these are briefly considered below.

High-Resolution X-Ray Telescope

The object of the experiment with a high-resolution X-ray telescope is to obtain X-ray spectroheliograms, particularly of plage regions, with a resolution of a few arc-seconds. The instrument will cover wavelengths from 6 Å to 60 Å: the 6–10-Å region should include radiation from flares, and the longer wavelengths are of interest for quiet-Sun and plage studies. The main instrument will use double-reflection grazing-incidence optics (fig. 2) with a large collecting area of several ten's of square centimeters. The X-ray image detector will consist of a thin scintillator, an image intensifier, fiber optics, and a television

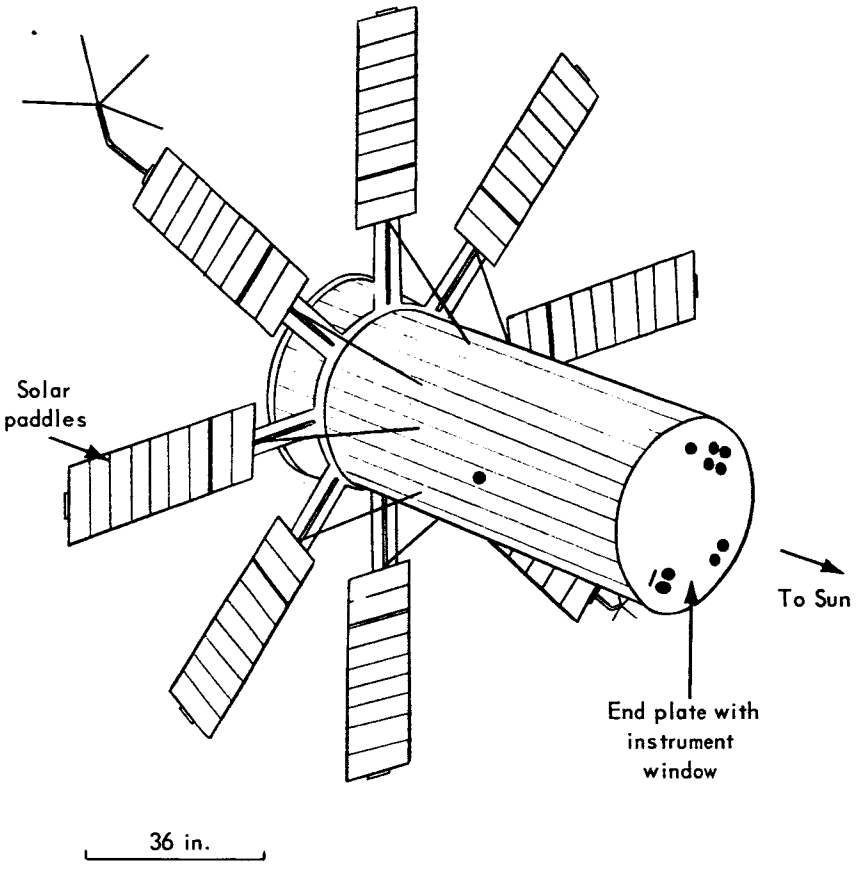

Figure 14.—**Advanced Orbiting Solar Observatory.**

camera. A square picture of 2.5×10^5 resolution bits is proposed. A second, low-resolution (1 arc-minute) telescope will also be used for fast time resolution of solar disturbances.

White Light Coronagraph

The White Light Coronagraph experiment (Eddy and Newkirk, HAO) is designed to record changes in brightness, extent, and polarization of the outer corona, both long term (days to months) and short term (minutes), with angular resolution of 1 arc-minute or less. The purpose of operating a high-resolution, white-light coronagraph in an Earth orbit is to obtain a nearly continuous patrol of the outer corona over a period of several months. High-resolution observations from an orbital corona-

graph would provide, for the first time, details of the changes occurring in the outer corona, which may be presumed to accompany many solar surface and radio events.

Spectroheliographs in Ultraviolet and Hydrogen Lyman-Alpha

The objectives of the spectroheliograph experiment (Purcell, Tousey, and Friedman, NRL) are to carry out spectroheliographic observations with high angular and wavelength resolution with the hydrogen Lyman-alpha line, and high angular resolution spectroheliographic observations using the entire emission line, for certain chromospheric and coronal lines. Only in the extreme ultraviolet can spectroheliographic observations be made with lines originating in the high chromosphere and corona. Observations from an orbiting observatory are required to follow into the high chromosphere and corona, the morphology and dynamic processes of solar events originating low in the Sun's atmosphere.

300 Å–1300 Å Scanning Spectroheliometer

The proposed spectroheliometer (Goldberg, Reeves, and Parkinson, HCO) will greatly improve the spatial resolution of the solar disk from about 1 arc-minute to 5 arc-seconds. The improved resolution should be good enough for studies of the fine structure of active regions and, possibly, of the nonhomogeneous structure of the chromosphere and corona. Spectroheliograms will also be obtained of areas 5 arc-minutes square with a spatial resolution of 5 arc-seconds at any desired wavelength in the 300-Å–1300-Å range.

Future flights should provide considerably more data on the distribution of ultraviolet and X-ray sources across the Sun and their correlation with visible and radio sources. The relatively sparse data on line spectra in the ultraviolet and X-ray region will be augmented by both rocket and satellite flights. The numerous X-ray monitors should enable flares and other disturbances to be observed in greater numbers and in more detail, while the continuation of measurements will extend through a maximum of the solar cycle.

FAR DISTANT FUTURE POSSIBILITIES

When technological advances permit such missions, a close vantage point for solar observation will naturally allow higher angular resolution than the largest feasible Earth-bound or Earth-orbiting telescopes. The technological areas requiring development are upper stage vehicle power and flight control; wide bandwidth communication (data and control telemetry) over the large distances involved; thermal protection for experiments and spacecraft subsystems; and high output power supplies to support the communication system.

Early feasibility studies have revealed the scope of engineering effort required to perform a minimum justifiable optical solar probe mission. The approximate resolution limit of ground solar telescopes is $\frac{1}{3}$ arc-second at 5000 Å. In the foreseeable future, an upper limit to Earth-orbiting solar telescope resolution might be $\frac{1}{40}$ arc-second (100-inch diffraction-limited objective at 2500 Å). Such a large-aperture telescope certainly will require manned supporting operations. At 0.2 AU from the Sun, a 20-inch telescope could achieve comparable angular resolution, and an instrument this size could conceivably operate on an unmanned mission. Despite its higher capital costs, a manned 100-inch telescope will offer a greatly extended lifetime of research utility compared to the few weeks operation of a probe near perihelion. On the other hand, the technological development required by a 100-inch manned telescope may come much later than needed by the solar probe.

Close-look telescopic observation is not the only special advantage of the probe. It would also permit back-of-Sun observations; however, these promise little new scientific knowledge. Moreover, it is not clear that such observations done on a patrol basis would materially improve the ability to forecast solar flares. The probe would also provide a unique opportunity for examining a single prominence simultaneously from two points of view—from Earth and from the probe. However, this feature is not a compelling reason to perform a probe experiment since solar rotation provides the essential information in a statistical way from many prominences.

In theory, observations closer than 1 AU to the Sun provide a gain in flux through a given telescope objective. Thus, the probe should increase signal-to-noise ratio, and in critical cases it might permit otherwise impossible observations, such as searching for some faint ultraviolet radiation expected during only one brief phase of a solar flare. A similar advantage relates to solar neutron studies from a probe: the average transit time through 1 AU of neutrons is comparable to their half-life. Therefore, the close-in probe should encounter a much greater increase of neutron flux than the inverse square law would indicate.

After reviewing the advantages and shortcomings of the close-in solar probe, the majority of solar astronomers have recommended that its application should be in the area of local measurements of the solar plasma. The energy spectra and flux of solar protons and M-region particle streams and the strength and direction of the associated magnetic fields can be discovered only by *in situ* measurements. The morphology of cosmic-ray modulation phenomena, and particularly the character of the interplanetary storm, continue to rank high in interest as space research objectives.

chapter 10

Summary and Conclusions

BY THE BEGINNING of the 6-year period, 1958 to 1964, the first attempts to examine the solar soft X-ray and ultraviolet spectrum had been made. During this period these measurements have been refined so that the whole spectrum is now known fairly accurately under quiet-Sun conditions. Measurements have also demonstrated the large variations in X-ray flux that occur during solar disturbances and the relation between these and ionospheric phenomena. Thus far, however, only the simpler aspects of these phenomena are understood, and a considerable extension of measurement techniques is needed to understand the numerous solar processes. Similarly, high wavelength and angular resolution have only recently been obtained in solar soft X-ray measurements, and much remains to be done. Some unresolved solar problems are briefly discussed below.

THERMODYNAMIC STRUCTURE

Great effort in solar physics is directed toward a knowledge of the thermodynamic parameters that govern the solar properties in both quiet and disturbed conditions. The simplifying assumptions of energy equilibrium established by radiative processes only, hydrostatic equilibrium and local thermodynamic equilibrium are not valid and there is considerable controversy over the magnitudes, and sometimes the direction, of departures from these assumptions. An example is the extremely rapid rise in electron temperature above the photosphere from about 5×10^3 °K at the photospheric surface to about 10^6 °K at altitudes above 10^4 kilometers. One of the crucial problems of the solar atmosphere is the nature of this nonradiative energy source and its possible connection with subphotospheric convection and the presence of wave disturbances.

209-916 O—66——7

GEOMETRIC STRUCTURE

Departures from equilibrium conditions are indicated by the presence of granulation, faculae and sunspots in the photosphere, together with a mottled appearance of the lower chromosphere. In addition, the upper chromosphere above about 3000 kilometers consists entirely of geyserlike spicules having a short lifetime. An accurate description of the detailed structure throughout the whole atmosphere presents another problem.

VELOCITY FIELDS

Mass movements in the solar photosphere and chromosphere have been detected by observations of the Doppler shift of spectral lines, but such results allow extremely wide ranges of interpretation. The energy transported in mass movements is extremely large, thus representing an important field for future study.

FLARES

The study of flares involves all the difficulties in understanding the quiet Sun together with the added complexity that flares are a time-dependent phenomena and are related to the production of large numbers of high-energy particles. Flare phenomena present a considerable challenge since they involve the whole electromagnetic spectrum down to hard X-rays and the particle spectrum from a few hundred eV to cosmic-ray energies.

CORONAL PHENOMENA

All observations show large-scale structure in the corona. Spectroscopic results, however, indicate additional small-scale structure. Some of these results might be considered further in connection with the study of heating mechanisms and of the degradation of mechanical energy. The type of analysis used for the transition-region ultraviolet spectrum could be extended to include X-ray, visible, and radio spectra. It would be desirable to have observations covering as wide a range of wavelengths as can be made at the same time.

Other problems are posed by the apparent differences in composition between the corona and the photosphere. While the

assumption of some departure from spherical symmetry is probably needed to interpret these data, this has not yet been conclusively demonstrated. At present not enough information is available to permit postulation of a two or more component atmosphere for the transition region. Further, accuracy must be improved, especially for white-light observations, which are important in determining the electron density.

SOLAR MAGNETIC FIELDS

Polarization of radio waves and the trajectories of some coronal and chromospheric features show that magnetic fields are present near the Sun. It would be of interest to know the field configurations in detail near the Sun and also further out. For this purpose, solar probes and magnetometer techniques would provide useful information.

FURTHER UNSOLVED PROBLEMS

Thus far in the measurement of solar soft X-ray and ultraviolet flux, the time-resolution limit of transient phenomena such as flares has been set by the detection instruments, and it would be desirable to improve resolution to better than 1 second. Such time resolution would give further information on the processes occurring during solar disturbances and on the volumes of material participating in the radiation emission.

Earthbound monitoring of solar radiofrequency radiation below 10 Mc/sec is limited by ionospheric absorption and reflection, but such monitoring has not yet been attempted from above the atmosphere.

References

1. MAYER, U.: Space Sci. Rev., vol. 3, 1964, p. 781.
2. ERGIN, E. I.: Progress in Astronautics and Astronomics. Vol. XIII. Academic Press, 1964, p. 3.
3. DOLDER, F. P.; BARTAE, O. E.; MERCURE, R. C., JR.; GABLEHOUSE, R. H.; AND LINDSAY, J. C.: Space Research III (W. Priester, ed.), North-Holland Pub. Co. (Amsterdam), 1963, p. 1207.
4. BURNIGHT, T. R.: Phys. Rev., ser. 2, vol. 76, 1949, p. 165.
5. BLAKE, R. L.; CHUBB, T. A.; FRIEDMAN, M.; AND UNZICKER, A. E.: Astrophys. J., vol. 137, 1963, p. 3.
6. POUNDS, K. A.; AND BOWEN, P. J.: Monthly Notes, Roy. Astron. Soc., vol. 123, 1962, p. 348.
7. POUNDS, K. A.: Ph. D. Thesis. University College, London, 1961.
8. ATKINSON, P. A.; AND POUNDS, K. A.: J. Phot. Sci., 1964.
9. KREPLIN, R. W.: Ann. Geophys., vol. 17, 1961, p. 19.
10. KREPLIN, R. W.; CHUBB, T. A.; AND FRIEDMAN, H.: J. Geophys. Res., vol. 67, 1962, p. 2231.
11. ACTON, L. W.; CHUBB, T. A.; KREPLIN, R. W.; AND MEEKINS, J. F.: J. Geophys. Res., vol. 68, 1963, p. 3335.
12. MANDEL'STAM, S. L.; TINDO, I. P.; VORON'KO, YU. K.; VASIL'YEV, B. N.; AND SURGYIN, A. I.: Planetary Space Sci., vol. 11, 1963, p. 61.
13. NEWELL, H. E.: High Altitude Rocket Research. Academic Press, 1953.
14. POUNDS, K. A.; AND WILLMORE, A. P.: Space Research III (W. Priester, ed.), North-Holland Pub. Co. (Amsterdam), 1963, p. 1195.
15. CULHANE, J. L.; POUNDS, K. A.; SANFORD, P. W.; AND WILLMORE, A. P.: Space Research IV (P. Muller, ed.), North-Holland Pub. Co. (Amsterdam), 1964, p. 741.
16. LUKIRSKII, A. P.; RUMSH, M. A.; AND SMIRNOV, L. A.: Opt. Spectr. (U.S.S.R.), English Transl., vol. 9, 1960; no. 4, p. 265; no. 5, p. 343.
17. YEFREMOV, A. I.; PODMOSHENSKIY, A. L.; IVANOV, M. A.; NIKIFOROV, V. N.; AND YEFIMOV, O. N.: Artificial Earth Satellites, vol. 10, 1961, p. 48.
18. RENTSCHLER, H.; HENRY, D.; AND SMITH, K. O.: Rev. Sci. Instr., vol. 3, 1932, p. 794.

19. DUNKLEMAN, LAWRENCE: Ultraviolet Photodetectors. NASA TN D–1718, 1963.
20. TAFT, E.; AND APKER, L.: J. Opt. Soc. Am., vol. 43, 1953, p. 81.
21. GOODRICH, G. W.; AND WILEY, W. C.: Experiments with the Bendix Continuous-Channel Multiplier. Image Intensifier Sym. NASA SP–2, 1962, pp. 211–213.
22. HUNTER, W. R.: Space Research III (W. Priester, ed.), North-Holland Pub. Co. (Amsterdam), 1963, p. 1187.
23. GOODRICH, G. W.; AND WILEY, W. C.: Rev. Sci. Instr., vol. 32, 1961, p. 846.
24. STERNGLASS, E. J.; AND FEIBLEMAN, W. A.: U.S. Patent No. 2,898,499, 1961.
25. CHUBB, T. A.; FRIEDMAN, H.; KREPLIN, R. W.; BLAKE, R. L.; AND UNZICKER, A. E.: Mem. Soc. Roy. Sci. Liege, Ser. 5, vol. 4, 1961, p. 228.
26. BAEZ, A. W.: J. Opt. Soc. Am., vol. 51, 1961, p. 405.
27. MOLLENSTEDT, G.; VOY GROTE, K. H.; AND JONSSON, C.: Paper presented at Third Intern. Symp. X-Ray Optics and X-Ray Microanalysis (Stanford), 1962 (Pattee, Gosslett, and Engstrom, eds.), Academic Press, 1963, p. 73.
28. HENKE, B. L.; AND MUELLER, W. M.: Advances in X-Ray Analysis. Vol. IV. Plenum Press (New York), 1961, p. 244.
29. GIACCONI, R.; GURSKY, H.; PAOLINI, F. R.; AND ROSSI, B. R.: Phys. Rev. Letters, vol. 9, 1962, p. 439.
30. GIACCONI, R.; HARMON, N. F.; LACEY, R. F.; AND SZILAGYI, Z.: An X-Ray Telescope. NASA CR–41, 1965.
31. GRAY, S.: Electronic UV Imaging Techniques. Proc. Natl. IAS–ARS Joint Meeting (Calif.), 1961.
32. BYRAM, E. T.; CHUBB, T.; AND FRIEDMAN, H.: Rocket Exploration of the Upper Atmosphere (R. L. F. Boyd, M. Seaton, and H. S. W. Massey, eds.), Pergamon Press, Ltd. (New York), 1954.
33. MANDEL'STAM, C. L.; TINDO, I. P.; VORON'KO, YU. K.; SURGYIN, A. I.; AND VASIL'YEV, B. N.: Planetary Space Sci., vol. 9, 1962, p. 977.
34. SAWYER, G. A.; JAHODA, F. C.; RIBE, F. L.; AND STRATTON, T. F.: J. Quant. Spectr. Radiative Transfer, vol. 2, 1962, p. 571.
35. NEUPERT, W. M.; BEHRING, W. E.; WHITE, W. A.; AND LINDSAY, J. C.: X–614–62–156, Goddard Space Flight Center, 1962.
36. TOUSEY, R.: Space Sci. Rev., vol. 2, 1963, p. 3.
37. PURCELL, J. D.; PACKER, D. M.; AND TOUSEY, R.: Space Research. North-Holland Pub. Co. (Amsterdam), 1960, pp. 581–589 and pp. 594–598.
38. DETWILER, C. R.; PURCELL, J. D.; AND TOUSEY, R.: Mem. Soc. Roy. Sci. Liege, Ser. 5, vol. 4, 1961, p. 254.
39. RENSE, W. A.: Phys. Rev., vol. 91, 1953, p. 299.

40. VIOLETT, T.; AND RENSE, W. A.: Astrophys. J., vol. 130, 1959, p. 954.
41. AUSTIN, W. E.; PURCELL, J. D.; AND TOUSEY, R.: Astron. J., vol. 67, 1962, p. 110.
42. HINTEREGGER, H. E.: Telemetering Monochromator Measurements of Extreme Ultra-violet Radiation. Space Astrophysics (W. Liller, ed.), McGraw-Hill, 1961, pp. 34–95.
43. PURCELL, J. D.; AND TOUSEY, R.: Mem. Soc. Roy. Sci. Liege, Ser. 5, vol. 4, 1961, p. 274.
44. DETWILER, C. R.; AND PURCELL, J. D.: J. Opt. Soc. Am., vol. 52, 1962, p. 597.
45. TOUSEY, R.: Quart. J. Roy. Astron. Soc., vol. 5, 1964, p. 123.
46. ALLEN, C. W.: Space Sci. Rev., vol. 4, 1965, p. 91.
47. HINTEREGGER, H. E.: Rocket Spectra of the Chromosphere. Paper presented at Symp. on the Solar Spectrum (Utrecht), Aug. 1963.
48. HALL, L. A.; DAMON, K. R.; AND HINTEREGGER, H. E.: Space Research III (W. Priester, ed.), North-Holland Pub. Co. (Amsterdam), 1963, pp. 745–771.
49. PURCELL, J. D.; GARRETT, D. L.; AND TOUSEY, R.: Space Research III (W. Priester, ed.), North-Holland Pub. Co. (Amsterdam), 1963, p. 781.
50. HINTEREGGER, H. E.; HALL, L. A.; AND SCHWEITZER, W.: Astrophys. J., vol. 140, 1964, p. 319.
51. ZIRIN, H.: Astrophys. J., vol. 140, 1964, p. 1332.
52. POTTASCH, S. R.: Space Sci. Rev., vol. 3, 1964, p. 816.
53. HOUSE, L. L.: Astrophys. J. Suppl. No. 81, vol. 8, 1964, p. 307.
54. GOLDBERG, L.; MULLER, E. A.; AND ALLER, L. H.: Astrophys. J. Suppl., vol. 5, no. 45, 1960, p. 1.
55. MORTON, D. C.; AND WIDING, K. D.: Astrophys. J., vol. 133, 1961, p. 596.
56. ZIRIN, H.; AND DIETZ, R. D.: Astrophys. J., vol. 138, 1963, p. 664.
57. POUNDS, K. A.; et al.: Proc. Roy. Soc. London, Ser. A, vol. 281, 1964, p. 538.
58. HULBERT, E. O.: Phys. Rev., vol. 53, 1938, p. 344.
59. VEGARD, L.: Geophys. Publ., vol. 12, 1938, p. 5.
60. EDLEN, B.: Z. Astrophysics, vol. 22, 1942, p. 30.
61. HOYLE, F.; AND BATES, D. R.: Terrest. Magnetism and Atmospheric Elec., vol. 53, 1948, p. 51.
62. FRIEDMAN, H.; LICHTMAN, S. W.; AND BYRAM, E. T.: Phys. Rev., vol. 83, 1951, p. 1025.
63. FRIEDMAN, H.: Rept. Progr. Phys., vol. 25, 1962, p. 163.
64. ELWERT, G.: J. Geophys. Res., vol. 66, 1961, p. 391.
65. STEIN, W. A.; AND NEY, E. P.: J. Geophys. Res., vol. 68, 1963, p. 65.
66. SCHKLOVSKY: Nature, vol. 202, 1964, p. 275.
67. ACTON, L. W.: X-Radiation of the Sun. Thesis, University of Colorado, 1964.

68. FRIEDMAN, H.; AND CHUBB, T. A.: Rept. of Conf. on Physics of the Ionosphere (Cambridge), 1954. Phys. Soc. (London), 1955, p. 58.
69. BLAKE, R. L.; CHUBB, T. A.; FRIEDMAN, H.; AND UNZICKER, A. E.: Science, vol. 146, 1964, pp. 1037–38.
70. PETERSON, L. E.; AND WINCKLER, J. R.: J. Geophys. Res., vol. 64, 1959, p. 697.
71. CHUBB, T. A.; FRIEDMAN, H.; AND KREPLIN, R. W.: J. Geophys. Res., vol. 65, 1960, p. 1831.
72. ANDERSON, K. A.; AND WINCKLER, J. R.: J. Geophys. Res., vol. 67, 1962, p. 4103.
73. SEATON, M. J.: 1964, Planetary Space Sci., vol. 12, 1964, p. 55.
74. DE JAGER, C.; AND KUPERUS, M.: Bull. Astron. Inst. Neth., vol. 16, 1961, p. 71.
75. LINDSAY, J. C.: AIAA Preprint 63–470, AIAA/CASI/RAeS 9th Anglo-American Conference, 1963.
76. WHITE, W. A.: Space Research IV (P. Muller, ed.), North-Holland Pub. Co. (Amsterdam), 1964, p. 771.
77. WHITE, W. A.: Planetary Space Sci., vol. 12, 1964, p. 379.
78. FROST, K. J.: Paper presented at COSPAR Symposium, May 1963.
79. NEUPERT, W. M.; BEHRING, W. E.; AND LINDSAY, J. C.: Space Research IV (P. Muller, ed.), North-Holland Pub. Co. (Amsterdam), 1964, p. 719.
80. NEUPERT, W. M.: Space Research IV (P. Muller, ed.), North-Holland Pub. Co. (Amsterdam), 1964, p. 731.
81. HALLAM, KENNETH L.: Solar Flares in the Light of Hydrogen Lyman-Alpha. AAS–NASA Symposium on the Physics of Solar Flares. NASA SP–50, 1964, pp. 63–64.

Articles of General Interest

HINTEREGGER, H.: Rocket Spectra of the Chromosphere. Paper presented at Symp. on the Solar Spectrum (Utrecht), 1963.

TOUSEY, R.: Extreme Ultraviolet Spectrum of the Sun. Space Sci. Rev., vol. 11, 1963, p. 3.

Report of Comm. 44: Observations au de hors l'Atmosphere Terrestre. IAU 12th General Assembly (Hamburg), 1964.

VAN DE HULST, H. C.; DE JAGER, C.; AND MOORE, A. F., EDS.: Space Research II. North-Holland Pub. Co. (Amsterdam), 1961.

PRIESTER, W., ED.: Space Research III. North-Holland Pub. Co. (Amsterdam), 1963.

ALLEN, C. W.: The Interpretation of the XUV Solar Spectrum. Space Sci. Rev., 1964.

FRIEDMAN, H.: Ultraviolet and X-rays From the Sun. Ann. Rev. Astron. Astrophys., vol. 1, 1963, p. 59.

IAU Symposium No. 23: Astronomical Observation From Space Vehicles, Liege, 1964.

GOLDBERG, L.: Space Astronomy. Proc. IAU 12th General Assembly, Hamburg, 1964.

TOUSEY, R.: George Darwin Lecture. Quart. J. Roy. Astron. Soc., vol. 5, 1963, p. 123.

BOYD, R. L. F.: Techniques for the Measurement of Extra-Terrestrial Soft X-Radiation. Space Sci. Rev., vol. 4, 1965, p. 35.

FRIEDMAN, H.: Solar Observations Obtained From Vertical Sounding. Rept. Progr. Phys., vol. 25, 1962, p. 163.

SMITH, H. J.; AND SMITH, E.: Solar Flares. Macmillan Co., 1963.

LINDSAY, J. C.: The Solar Extreme Ultraviolet Radiation (1–400 Å). Planetary Space Sci., vol. 12, 1964, p. 379.

U.S. GOVERNMENT PRINTING OFFICE: 1966 O—209-916

"The aeronautical and space activities of the United States shall be conducted so as to contribute . . . to the expansion of human knowledge of phenomena in the atmosphere and space. The Administration shall provide for the widest practicable and appropriate dissemination of information concerning its activities and the results thereof."

—NATIONAL AERONAUTICS AND SPACE ACT OF 1958

NASA SCIENTIFIC AND TECHNICAL PUBLICATIONS

TECHNICAL REPORTS: Scientific and technical information considered important, complete, and a lasting contribution to existing knowledge.

TECHNICAL NOTES: Information less broad in scope but nevertheless of importance as a contribution to existing knowledge.

TECHNICAL MEMORANDUMS: Information receiving limited distribution because of preliminary data, security classification, or other reasons.

CONTRACTOR REPORTS: Technical information generated in connection with a NASA contract or grant and released under NASA auspices.

TECHNICAL TRANSLATIONS: Information published in a foreign language considered to merit NASA distribution in English.

SPECIAL PUBLICATIONS: Information derived from or of value to NASA activities. Publications include conference proceedings, monographs, data compilations, handbooks, sourcebooks, and special bibliographies.

TECHNOLOGY UTILIZATION PUBLICATIONS: Information on technology used by NASA that may be of particular interest in commercial and other nonaerospace applications. Publications include Tech Briefs; Technology Utilization Reports and Notes; and Technology Surveys.

Details on the availability of these publications may be obtained from:

SCIENTIFIC AND TECHNICAL INFORMATION DIVISION

NATIONAL AERONAUTICS AND SPACE ADMINISTRATION

Washington, D.C. 20546